

546343

**SANDIA NATIONAL LABORATORIES
WASTE ISOLATION PILOT PLANT**

**Recommendation for the Lower Limit of the Waste Shear Strength
(Parameter BOREHOLE : TAUFAIL)**

Revision 1

Author: Courtney G Herrick (6711) *Courtney G Herrick* 6/25/07
Print Signature Date

Author: Michael Riggins (6711) *Write for Mike Riggins* 6/25/07
Print Signature Date

Author: Byoung Yoon Park (6711) *Byoung Yoon Park* 6/25/07
Print Signature Date

Technical Review: Daniel J Clayton (6711) *DJ Clayton* 6/25/07
Print Signature Date

QA Review: Mario Chavez (6710) *Mario Chavez* 6/25/07
Print Signature Date

Management Review: Moo Y. Lee (6711) *Moo Y. Lee* 6/25/07
Print Signature Date

Executive Summary

This paper represents an assessment of the waste shear strength parameter TAUFAIL used in the computer program CUTTINGS_S. The current values as given in the performance assessment parameter database are:

Material	Property	Distribution	Range	Description
Borehole	TAUFAIL	Log-uniform	0.05 – 77.0 Pascals	Effective shear strength for erosion of waste.

Based on a detailed literature review, additional analysis, and experimental results on surrogate waste materials we propose the following changes be made to TAUFAIL in the performance assessment parameter database:

Material	Property	Distribution	Range	Description
Borehole	TAUFAIL	Uniform	1.50 – 77.0 Pascals	Effective shear strength for erosion of waste.

Information Only

Table of Contents

EXECUTIVE SUMMARY	2
TABLE OF CONTENTS.....	3
LIST OF TABLES	4
LIST OF FIGURES	5
1 Introduction	7
2 History of the Value of the Lower Limit of TAUFAIL	7
3 Erosion of Soft Cohesive Sediments	8
3.1 Characteristics of Soft Cohesive Sediment Erosion	8
3.2 Analysis of Partheniades (1965) Erosion Tests	13
3.3 Operational Critical Shear Stress	18
3.4 Recommendation for the Waste Shear Strength Value.....	19
4 Review of Analysis Based on Expert Panel's Particle Distribution.....	21
5 Tests on Surrogate Waste Materials.....	23
6 Waste Permeability and the Possibility of Stuck Pipe / Gas Erosion.....	35
7 Summary and Recommendation	37
7.1 Summary	37
7.2 Recommendation	39
8 References	39

List of Tables

Table 3-1.	Erosion test results from Parchure and Mehta (1985, Table 1).	12
Table 3-2.	Summary of erosion rates from Partheniades (1965, Tables 1, 5, and 6).	15
Table 3-3.	Summary of shear strengths from present analysis and Partheniades (1965).	18
Table 4-1.	Critical shear stress of WIPP waste calculated as a function of waste mean particle diameter (Wang and Larson 1997, Table 2).	22
Table 5-1.	Average erosion rates (cm/sec) for each shear stress (dyne/cm ²) (Jepsen et al. 1998, Table 1)	26
Table 5-2.	Critical shear stresses for each sample as determined by Jepsen et al. (1998, Table 2)	27
Table 5-3.	Summary of shear strengths from present analysis and Jepsen et al (1998).	28
Table 7-1.	Compilation of results from various analyses conducted in this analysis.	38
Table 7-2.	Statistics for the parameter BOREHOLE : TAUFAIL to be entered into the parameter database:	39

List of Figures

Figure 3-1.	Variation of (a) density and (b) shear strength with depth of a kaolinite sediment bed in salt water. (Parchure and Mehta 1985, Figures 3 and 4.).....	10
Figure 3-2.	Schematic representation of three-zoned description of bed shear strength profile. (Parchure and Mehta 1985, Figure 5.)	10
Figure 3-3.	Concentration $C(t)$ at the end of each time step versus bed shear stress, τ_b , for a kaolinite sediment bed in salt water. Illustrated are the definitions of bed surface shear strength, τ_{so} , and characteristic shear strength of the bed, τ_{sc} . (Modified from Parchure and Mehta 1985, Figure 6).....	11
Figure 3-4.	Variation of bed shear strength with depth for SF Bay mud (Teeter 1987, App. B, Fig. 32) based on the procedure in Parchure and Mehta (1985).	13
Figure 3-5.	Reproduction of erosion rate versus shear stress plots for Series I and II tests (Partheniades 1965, Figure 7; Partheniades and Paaswell 1970, Figure 1).	16
Figure 3-6.	Plot of Series I rate of erosion versus average shear stress (data from Partheniades 1965).	17
Figure 3-7.	Plot of Series II rate of erosion versus average shear stress (data from Partheniades 1965).....	17
Figure 3-8.	Plot of Series III data from Partheniades (1965) for bottom shear stress versus rate of erosion. Original data is shown by solid dark blue diamonds and average erosion rates at each bottom shear stress level are depicted by open violet squares. The above figure does not represent a piecewise linear fit, but two separate linear fits.	18
Figure 3-9.	Concentration $C(t)$ at the end of each time step versus bed shear stress, τ_b , for a kaolinite sediment bed in salt water. Illustrated is the definition of the operational or design shear strength of the bed, τ_c . (Modified from Parchure and Mehta 1985, Figure 6).....	19
Figure 3-10.	Schematic of various shear strengths and the direction of the currents acting on them: (a) flume experiment and (b) WIPP repository.	20
Figure 5-1.	Piecewise linear fit to data from Sample B2 (Jepsen et al. 1998) to obtain bed surface shear strength (τ_{so}) and bed characteristic shear strength (τ_{sc}).	29
Figure 5-2.	Linear fit to data of Sample B2 (Jepsen et al. 1998) after which the erosion rate increases sharply to obtain the operational shear strength τ_c	29
Figure 5-3.	Linear fit to all the data of Sample B3 (Jepsen et al. 1998) to obtain the operational shear strength τ_c	30
Figure 5-4.	Linear fit to all the data of Sample B4 (Jepsen et al. 1998) to obtain the operational shear strength τ_c	30

Figure 5-5.	Plot of data from Sample B5 (Jepsen et al. 1998). Test series was stopped at one shear stress level because flow meter was destroyed by debris at the next shear stress level.	31
Figure 5-6.	Plot of data from Sample B6 (Jepsen et al. 1998). Like Jepsen et al (1998), present analysis uses lowest value reported for shear stress causing erosion. See Note d of Table 5-1.	31
Figure 5-7.	Piecewise linear fit to data from Sample B7 (Jepsen et al. 1998) used to obtain bed surface shear strength (τ_{so}), operational shear strength (τ_c), bed characteristic shear strength (τ_{sc}).....	32
Figure 5-8.	Piecewise linear fit to data from Sample B8 (Jepsen et al. 1998) used to obtain bed surface shear strength (τ_{so}), operational shear strength (τ_c), bed characteristic shear strength (τ_{sc}).....	32
Figure 5-9.	Piecewise linear fit to data from Sample B9 (Jepsen et al. 1998) used to obtain bed surface shear strength (τ_{so}), operational shear strength (τ_c), bed characteristic shear strength (τ_{sc}).....	33
Figure 5-10.	Iron remaining in WIPP from present recertification calculations for the undisturbed scenario.	34
Figure 5-11.	Iron remaining in WIPP from present recertification calculations for the E1 scenario at 350 years as the worst case.....	34
Figure 6-1.	Porosity of waste as a function of time for the cases of $f = 0.0$ with only salt creep considered and $f = 0.2$ considering loading and secondary compression (Herrick et al. 2007).	36

1 Introduction

Waste Isolation Pilot Plant (WIPP) Performance Assessment (PA) scenarios include cases of human intrusion in which a future drilling borehole intersects the waste in the repository. Drilling mud flowing up the borehole will apply a shear stress to the borehole wall which if high enough, could result in erosion of the wall material (Berglund 1992). This eroded volume is called “cavings,” whereas the volume of the material removed by the drill bit is called “cuttings”. Both processes could result in a release of radionuclides.

WIPP PA uses the parameter BOREHOLE : TAUFAIL to represent the waste shear strength in the numerical code CUTTINGS_S. (see WIPP PA 2004a, 2004b, 2005a, 2005b for a thorough description of the CUTTINGS_S code). The parameter is currently a sampled value using log-uniform distribution with a range of 0.05 to 77 Pa. This range of values was derived by DOE from literature reviews of erosion of a bay mud and consideration of the mean particle size of WIPP waste (Berglund 1996, Wang and Larson 1997). The lower limit of this range of values was chosen to conform to what is hypothesized as an extreme case of degradation of the waste and waste containers.

This report reexamines the lower limit value of BOREHOLE : TAUFAIL according to the manner outlined in the planning document AP-131, Rev. 0 (Kirkes and Herrick 2006). This revision is a result of apprehension expressed during a technical exchange with the EPA on May 23, 2007 about the validity of SANTOS calculations used in the initial analysis report version. After that exchange, it was decided that in order to adequately address the concerns about SANTOS calculations a new plasticity model for the waste’s structural behavior would have to be developed. This analysis, therefore, stresses the results of erosion experiments performed on surrogate waste materials in order to assess the parameter’s lower value.

In Section 2, a brief history of how the lower limit of the waste shear strength was obtained is provided. Section 3 discusses concepts and definitions used in erosion studies of ocean and channel bed sediments. Section 4 revisits the findings of the expert panel on mean particle sizes in WIPP. Section 5 discusses the results of experiments performed on surrogate waste materials. In Section 6 we briefly discuss the possibility of stuck pipe or gas erosion occurring. Section 7 presents a summary, conclusions, and recommendation for the value of the lower limit of the waste shear strength.

2 History of the Value of the Lower Limit of TAUFAIL

J. Berglund (1992) performed the first analyses and created the original models for cuttings, cavings, and spalling for the WIPP purposes. Berglund assumed that:

In the absence of experimental data, the effective shear strength for erosion of the repository material is assumed to be similar to that of a montmorillonite clay, with an effective shear strength of 1 to 5 Pa (Sargunam et al., 1973).

Butcher (1994) argued from a mechanical standpoint that the degraded waste would be similar to a clay-sand mixture. Based on literature values, he estimated that the strength of such a mixture would range between 0.1 and 1 Pa, with a median value of 0.5 Pa. Later, Butcher et al. (1995) changed the range to 0.1 to 10 Pa with a median of 1 Pa using a constructed distribution, again based on their literature review.

For the Compliance Certification Application (CCA), the DOE (1996) assumed a uniform distribution of the waste shear strength with a range of 0.05 to 10 Pa and a median of 5.0 Pa. This range was based on studies using soft mud, i.e., San Francisco Bay mud (Berglund 1996). The Berglund memorandum simply reports the range of data for an ocean-bay mud (Partheniades and Paaswell 1970) and montmorillonite clay (Sargunam et al. 1973).

The sensitivity of the Cavings Model to changes in the waste shear strength was studied by the EPA as part of their evaluation for the Performance Assessment Validation Test (PAVT) (Trovato 1997a). They found that the cavings model is sensitive to the values chosen for TAUFAIL, in particular the lower limit as a weaker material would result in greater cavings release. As a result, the EPA required the DOE to change its method for estimating the waste shear strength and use an estimation based on particle size distributions instead of analog experimental data as was done for the CCA (Trovato 1997b).

For the PAVT, the waste shear strength was estimated based on particle size distributions determined by an expert elicitation panel. The estimates used the Shield's parameter, which relies on a measure of the central point of a population of particles of different sizes, to determine the critical shear stress for an erodible, cohesionless sediment bed. With this approach, the calculated critical shear strength ranged from 0.64 to 77 Pa (Wang 1997, Wang and Larson 1997). For conservatism, the lower limit from the CCA was retained for the PAVT while the high value from the Shield's parameter method was used for the high value of the PAVT (EPA 1998). A log-uniform distribution for the waste was selected for the PAVT to provide equal weighting over the three orders of magnitude in the range.

Thus, WIPP PA calculations currently use a range of 0.05 to 77 Pa and a log-uniform distribution.

3 Erosion of Soft Cohesive Sediments

3.1 Characteristics of Soft Cohesive Sediment Erosion

Mehta et al. (1982) and Parchure and Mehta (1985) discuss the erosion characteristics of soft cohesive sediments. They differentiate between two bed types commonly used in erosion testing of sediments: placed beds and deposited beds. Placed beds are mechanically placed in the flume's sample holder and are considered to be representative of fully consolidated deposits. Deposited beds are those that are emplaced in the flume by the deposition and settling of sediments out of the flow of a current. They are stratified with respect to their properties with depth. Both placed and deposited beds can exhibit two modes of failure. The first, known as "surface erosion," involves particle by particle or aggregate by aggregate entrainment of the

surficial sediments. The second, known as “bed erosion,” results from shear loading of the bed. In this case, the plane of failure is deeper into the bed and erosion takes place by the removal of relatively large pieces of soil. This is the same observation made by Partheniades and Paaswell (1970, p 763) who refer to these two types of erosion as “surface erosion” and “mass erosion.”

Resistance to erosion is characterized by the properties of the bed. The erosion or resuspension potential of a bed is dependent of the mode of formation of the bed. In a natural environment, the bed forms as a result of particles settling out of the water column and being deposited on the bed. The degree of aggregation in a settling sediment influences the structure of the deposit. Aggregates in a freshly deposited bed are often composed of fluffy, weak units in comparison with settled aggregates. As consolidation proceeds, the interstitial water is expelled, the aggregates in layers below the surface compact, and comparatively stronger, more tightly packed units result. The bed becomes stratified and the aggregate shear strength and density typically increase monotonically with depth. When consolidation is allowed for a period of several days to months, the shear strength and the density distributions become invariant, and the bed acquires more uniform properties (e.g., Mehta et al. 1982, Jepsen et al. 1997, Roberts et al. 1998). Placed beds, by virtue of the manner in which they are prepared, are more representative of fully consolidated beds.

A common feature of placed beds is that the rate of surface erosion becomes constant or nearly constant after a short initial period of relatively more rapid erosion. The constant rate of erosion under a constant shear stress results because the shear strength of the bed varies little with depth. The erosion rate for deposited beds typically decreases as erosion proceeds, eventually reaching a constant value or even arresting. This resuspension behavior of deposited beds is explained when it is recognized that, by virtue of its manner of formation, the aggregate shear strength of the deposited bed increases measurably with depth due to settling of the sediments and consolidation of the sediments. The upper, surficial layer is soft with a high water content, often in excess of 100%, and low aggregate shear strength. Upon consolidation, the flocs or aggregates breakup and the particles undergo some rearrangement and settling causing the bed density and shear strength to increase with both depth and time. The increase in bulk density is associated with a decrease in porosity and water content.

In their erosion tests on kaolinite and lake mud deposited beds, Parchure and Mehta (1985) defined a number of characteristics of the beds that vary with depth and time. (The mud they tested was composed of montmorillonite, illite, kaolinite, and quartz.) Figure 3-1 shows an example of the variation of density, expressed in terms of concentration or weight of sediment solids per volume of sampled water, and shear strength with depth for kaolinite eroded in salt water. As expected from the foregoing discussion, both the density and shear strength increase with depth. They idealized the increase in shear strength with depth in Figure 3-2 in terms of three zones. The value of the shear strength, τ_s , at $z = 0$, τ_{so} , is for incipient motion of the bed. Incipient motion is the threshold condition between erosion and sedimentation of a single particle (Julien 1998). For example the Shield's Diagram (discussed in detail in Section 4) is a nondimensional plot of incipient motion shear stress values. Zone 1 has a thickness z_c that is bounded by τ_{so} at $z = 0$ and τ_{sc} at $z = z_c$. Zone 2 has a thickness z_d and is bounded by τ_{sc} at $z = z_c$ and τ_{sm} at $z = z_c + z_d$. An important difference between Zones 1 and Zone 2 is that the gradient $\delta\tau_s/\delta z$ is much larger in Zone 1 than that in Zone 2. Below z_d , in Zone 3, the shear strength of the bed is nearly constant, τ_{sm} and $\delta\tau_s/\delta z \approx 0$.

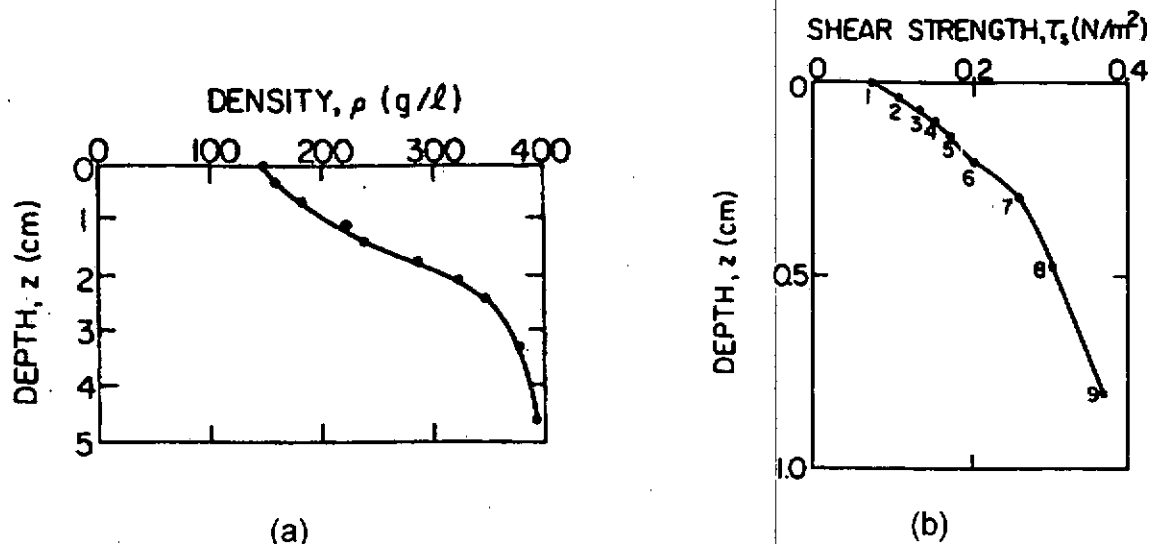


Figure 3-1. Variation of (a) density and (b) shear strength with depth of a kaolinite sediment bed in salt water. (Parchure and Mehta 1985, Figures 3 and 4.)

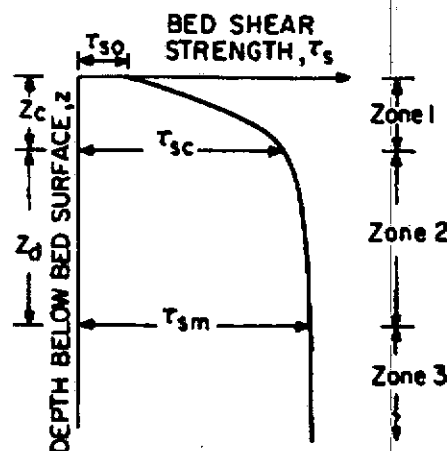


Figure 3-2. Schematic representation of three-zoned description of bed shear strength profile. (Parchure and Mehta 1985, Figure 5.)

Both τ_{so} and τ_{sc} can be estimated from a plot of eroded mass per unit surface area per unit time (erosion rate, ε) versus the bed shear stress, τ_b (Teeter 1987) or from a plot of suspended sediment concentration at the end of each incremental time step in the testing process $C(t)$ versus τ_b (Parchure and Mehta 1985). Figure 3-3 shows a plot of $C(t)$ versus τ_b from Parchure and Mehta (1985) for three different lengths of consolidation time. It is typically possible to approximate the data by two linear segments. The first segment is extrapolated to intersect the $C(t) = 0$ axis. The point where the line crosses the bed shear stress axis is τ_{so} . The point at which the two linear segments intersect corresponds to τ_{sc} . For all $\tau_b < \tau_{sc}$, the rate of erosion is low compared to that of $\tau_b > \tau_{sc}$. In most cases, investigators studying erosion of sediments are

interested in τ_{so} and/or τ_{sc} , and not τ_{sm} . For instance, see the data from Parchure and Mehta (1985) reproduced in Table 3-1.

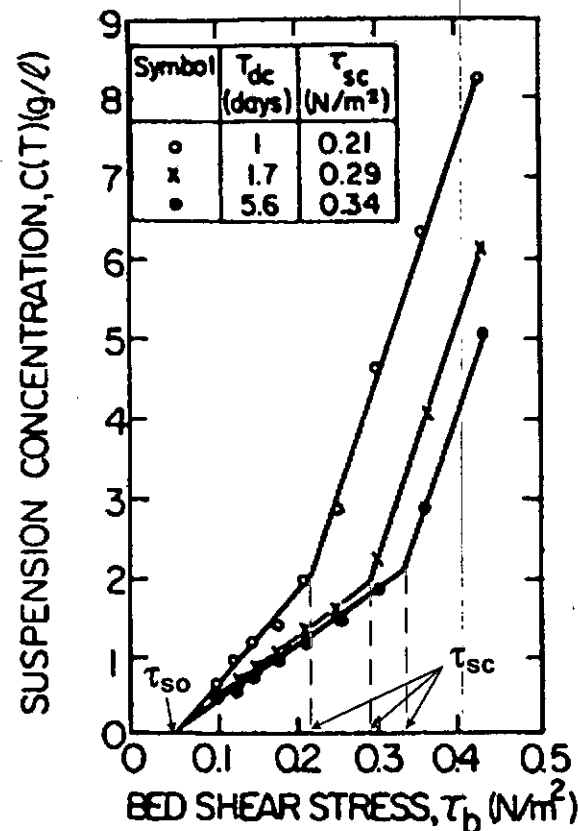


Figure 3-3. Concentration $C(t)$ at the end of each time step versus bed shear stress, τ_b , for a kaolinite sediment bed in salt water. Illustrated are the definitions of bed surface shear strength, τ_{so} , and characteristic shear strength of the bed, τ_{sc} . (Modified from Parchure and Mehta 1985, Figure 6)

A couple of observations can be made regarding the test results in Table 3-1. The first is that the present value of TAUFAIL chosen for San Francisco Bay mud is indeed on the conservative side of the range of values of other muds, but is still within the range typically found. Second, we see that Zone 1 is only a surface effect. It extends to a maximum depth of 0.40 cm (0.16 in). In tests conducted by Villaret and Paulic at the University of Florida on San Francisco Bay muds for the Army Corps of Engineers, the extent of Zone 1 is less than 0.2 cm (Figure 3-4). This is based on an estimate from the figures of that report (Teeter 1987, App. B, Figures 30 and 32) and applying the method described in Parchure and Mehta (1985). That method involves iteratively solving the following:

$$\Delta z = \frac{h}{\rho(z)} \Delta C \quad (3-1)$$

for each increase in shear stress of the flume. In this equation Δz is the change in depth with each increase, h is the water flow depth in the flume, $\rho(z)$ is the bed dry density at depth z , and ΔC is the change in suspension concentration associated with each increase in shear stress. Again, Zone 1 only represents the shear strength of the top layer of the bed. It is for this reason Villaret and Paulic refer to τ_{so} as “bed surface shear strength” (Teeter 1987, App. B). The value of $\tau_{AUFAIL} = 0.05$ Pa, in the present nomenclature is the surface bed shear strength, τ_{so} , as calculated by Partheniades and Paaswell (1970) using their expression. It is the value of incipient particle motion of this surficial layer. Mehta et al. (1982) and Parchure and Mehta (1985) conclude that the thickness of Zone 1 is on the order of millimeters in their experiments and that “in moderate tidal environments, such as costal Florida, maximum bed erosion during typical tidal conditions is found to be limited to a few centimeters.”

Table 3-1. Erosion test results from Parchure and Mehta (1985, Table 1).

Series ^a	Salinity (ppt)	T_{dc} (days)	τ_{so} (Pa)	τ_{sc} (Pa)	z_c (cm)	$\bar{\tau}_s$ (Pa)
LM	0.5	1.7	0.08	0.21	0.09	0.16
LM	1	1.7	0.12	0.27	0.07	0.24
LM	2	1.7	0.17	0.33	0.05	0.28
LM ^b	5	1.7	0.17	0.40	0.12	0.34
LM	10	1.7	0.17	0.62	0.17	0.39
KS	35	1.0	0.04	0.21	0.40	0.15
KS	35	1.7	0.04	0.29	0.30	0.22
KS	35	3.0	0.04	0.33	0.32	0.23
KS	35	5.6	0.04	0.34	0.26	0.33
KS	35	10.0	0.04	0.40	0.16	0.37
KT	0	1.0	0.10	0.30	0.16	0.23
KT	0	2.0	0.10	0.30	0.11	0.23
KT	0	3.0	0.10	0.35	0.03	0.26

Notes: T_{dc} is the time the beds were allowed to consolidate

$\bar{\tau}_s$ is the shear stress averaged over the thickness of Zone 1, z_c

^a Series defined as: LM – Lake Mud, KS – Kaolinite in Salt water, and KT – Kaolinite in Tap (fresh) water

^b Values were approximated due to insufficient data

The value τ_{sc} is called by Mehta et al. (1982) and Villaret and Paulic (Teeter 1987, App. B) the “characteristic shear strength” of the bed. It is the shear strength of the bed at the beginning of Zone 2. Laboratory results presented in Partheniades and Paaswell (1970), Mehta et al. (1982), Parchure and Mehta (1985), Teeter (1987), and many others demonstrate that the critical shear stress increases rapidly through Zone 1, but below this layer the rate of increase of the critical shear stress decreases at a much slower rate until becoming almost invariant with depth at a level τ_{sm} . The value τ_{sc} demarks the lower value of that time in which the critical shear stress trends toward becoming a constant (Figure 3-2). According to Mehta et al. (1982) and Parchure and

Mehta (1985) the extent of Zones 1 and 2 is on the order of centimeters, so the extent Zone 2 is relatively quite small also.

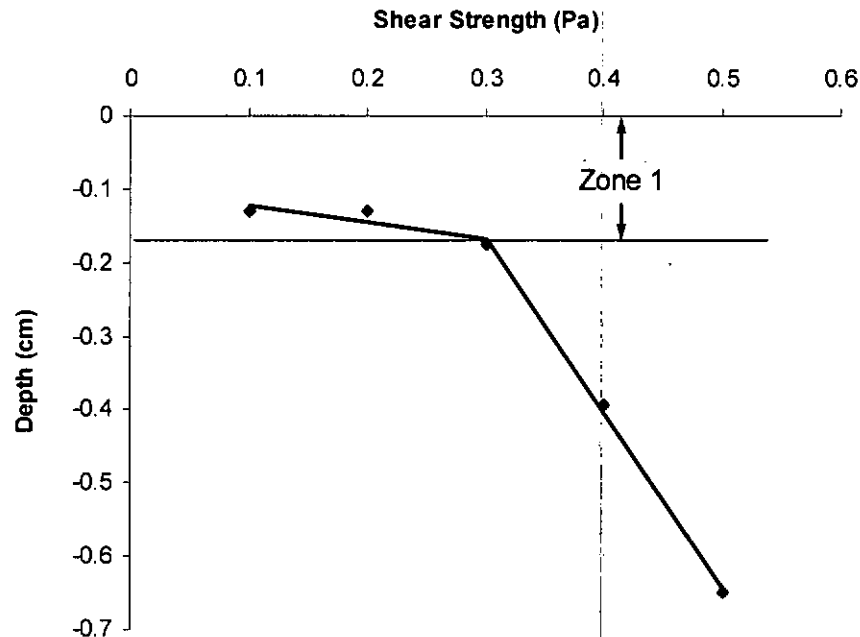


Figure 3-4 Variation of bed shear strength with depth for SF Bay mud (Teeter 1987, App. B, Fig. 32) based on the procedure in Parchure and Mehta (1985).

3.2 Analysis of Partheniades (1965) Erosion Tests

The current value of the lower limit of TAUFAIL was obtained from erosion test results reported in Partheniades and Paaswell (1970). The experimental work performed by Partheniades (1962, 1965) formed the basis for this paper. In this section we reanalyze his results by the method proposed by Parchure and Mehta (1985), as discussed in the last section.

Partheniades conducted erosion and deposition studies on a bed of clay which was referred to as "San Francisco Bay Mud." The mud is described as:

1. Classification: bluish-gray clay, high plasticity with some organics, falls between CH and OH in Unified Soil Classification System, principal mineral is montmorillonite with some illite.
2. Grain size: Clay ($< 2 \mu\text{m}$) $\approx 60\%$ by weight, Silt ($2 \mu\text{m}$ to $50 \mu\text{m}$) $\approx 40\%$ by weight, and fine sand small amount.
3. Atterburg limits: $w_H = 99\%$, $w_{pl} = 44\%$, and $PI = 55\%$
4. Natural water content: $w_n = 110\%$
5. Natural dry density: 40 lbs/ft^3

6. Shear strength: Remolded laboratory vane ultimate shear strength was 26 lb/ft^2 (0.18 psi, 1245 Pa). Flocculated shear strength was estimated to be between $1/136$ to $1/12$ of remolded strength, with an average of not more the $1/100$ of the remolded strength (0.0018 psi, 12.4 Pa).

Two types of test beds were considered. The first type was a 0.1 ft thick placed bed made of natural material (remolded mud) at the natural moisture content. This type of test bed was used for Series I and II tests. During the Series I tests a deep narrow groove of width b_m developed in the bed which ran the length of the flume. The rest of the test bed remained relatively flat but had a "crust" of possibly coarser grained material. Series II tests involved removing the crust and remolding the bed. In the process the moisture content of the bed increased slightly to 120%. For the Series II tests an erosion pattern similar to the Series I tests also formed, i.e., a narrow groove was formed in the bed that ran the length of the flume. However, a crust was not observed possibly because the flow rates were kept high in an attempt to prevent the deposition of fine sand. The second type was a deposited test bed that consisted of the same material used in the first type however the material was put into suspension and then allowed to settle out to create a "flocculated" bed. This test bed was 0.15 ft thick and was used for the Series III tests. It is uncertain as to the type of erosion pattern developed, since values for the width of the groove were not given. A summary of Partheniades (1965) test results are given in Table 3-2.

Table 3-2. Summary of erosion rates from Partheniades (1965, Tables 1, 5, and 6).

Series I Erosion Rates						
Run No.	Average Velocity (ft/sec)	Average Shear Stress		Estimated Rate of Erosion (g/ft²)/hour		Erosion width (b_m in feet)
		lbs/ft²	Pa	Initial	Final	
2	0.80	0.0023	0.110	0.050	0.050	0.550
3	1.34	0.0103	0.492	0.338	0.338	0.550
4	1.13	0.0070	0.334	0.170	0.170	0.550
5	0.95	0.0045	0.215	0.096	0.096	0.550
6	0.80	0.0023	0.110	0.050	0.050	0.550
9	1.48	0.0125	0.538	—	0.720	0.195
10	1.90	0.0195	0.934	1.670	1.670	0.195
11	2.34	0.0278	1.330	2.820	1.670	0.195
Series II Erosion Rates						
Run No.	Average Velocity (ft/sec)	Average Shear Stress		Estimated Rate of Erosion (g/ft²)/hour		Erosion width (b_m in feet)
		lbs/ft²	Pa	Initial	Final	
22	1.32	0.0100	0.478	0.174	—	0.33
23	2.31	0.0272	1.300	0.674	—	0.33
24	2.80	0.0383	1.880	2.160	—	0.33
25	3.22	0.0592	2.830	6.250	—	0.33
Series III Erosion Rates						
Run No.	Average Velocity (ft/sec)	Average Shear Stress		Estimated Rate of Erosion (g/ft²)/hour		Erosion width (b_m in feet)
		lbs/ft²	Pa	Initial	Final	
26	0.87	0.0032	0.153	0.165	0.041	—
27	1.07	0.0060	0.286	0.750	0.138	—
28	1.27	0.0091	0.435	0.506	0.506	—
29	1.07	0.0060	0.286	0.156	0.046	—
30	1.27	0.0091	0.435	0.166	0.009	—
31	1.46	0.0120	0.574	—	0.252	—
32	1.46	0.0120	0.574	0.252	0.252	—

The Series I and II test results are reproduced in Figure 3-5. The Series III data, the settled or flocculated bed, were not plotted in the original papers. Subsequent analysis by the present authors showed data scatter.

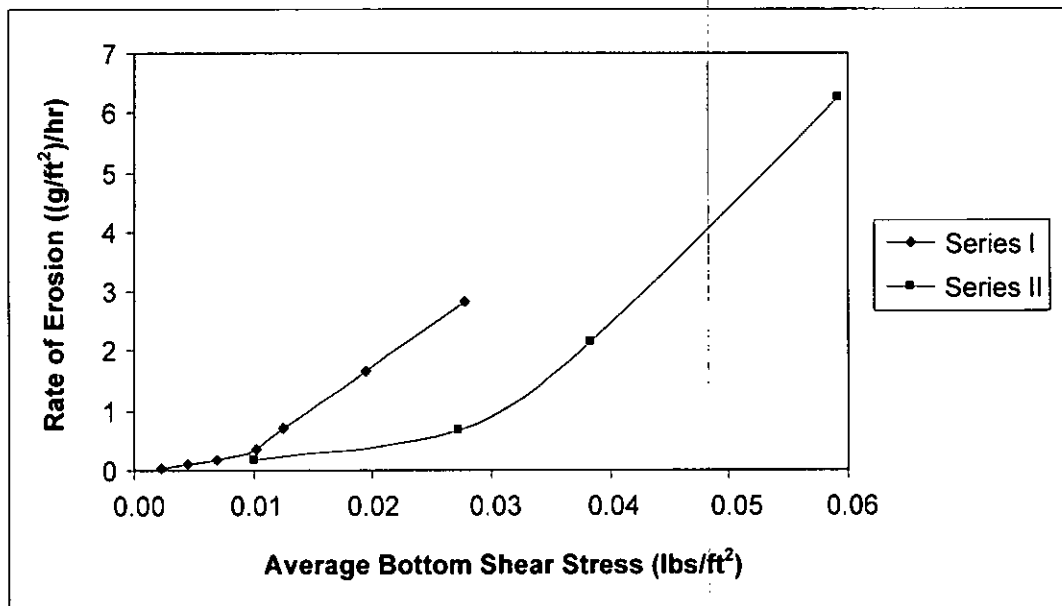


Figure 3-5. Reproduction of erosion rate versus shear stress plots for Series I and II tests (Partheniades 1965, Figure 7; Partheniades and Paaswell 1970, Figure 1).

Based on the test data and Figure 3-5, Partheniades (1965) made the following observations:

1. Initiation of scouring was first noticed at a velocity of 0.80 fps (which corresponds to a shear stress of 0.110 Pa) (pg. 112), [the author later states it is estimated to be the range of 0.65 to 0.80 fps. (pg. 122)]
2. There is a critical value of shear stress above which erosion rates increase much more rapidly with τ than below the critical value. For Series I this critical value was 0.010 lb per sq ft (0.48 Pa) and for Series II it was 0.028 lb per sq ft (1.34 Pa) (pg 124)
3. From a comparison of the results of Series I, II, and III it was found that the minimum scouring shear stress for dense and deposited bed were approximately the same and equal to 0.57 dynes per sq cm (0.057 Pa). (pg 127).

The data are replotted individually in order to better assess the shear stress parameters as discussed in the previous section. Figure 3-6 and Figure 3-7 represent the Series I and Series II data, respectively. A piecewise linear curve is fit to the data to determine the intercept (bed surface shear strength, τ_{so}) and intersection (characteristic shear strength, τ_{sc}) of the curves. The piecewise linear curve fits give good representations of the Partheniades data in both figures. Using the above data and plots, a summary of the shear strength parameters are given in Table 3-3. These are compared with Partheniades' (1965) analyses. Differences between the present analyses and Partheniades' are a result of the curve fitting methods used to analyze the data. In the present analyses the data were fit with a piecewise linear curve whereas Partheniades fit his data to a smooth function. Partheniades does not indicate how he chose his values for τ_{so} or τ_{sc} .

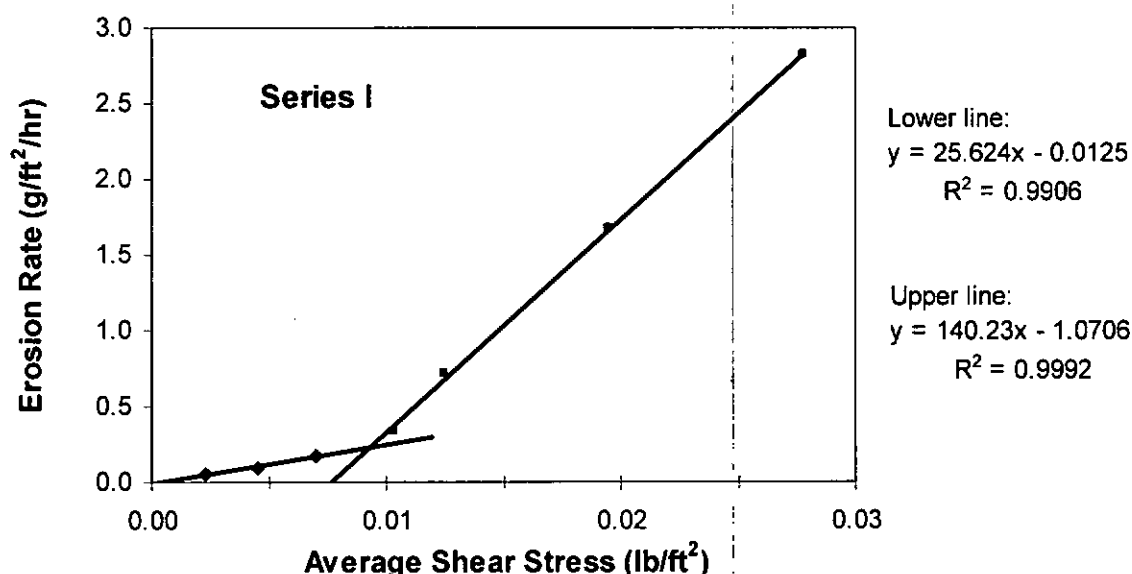


Figure 3-6. Plot of Series I rate of erosion versus average shear stress (data from Partheniades 1965).

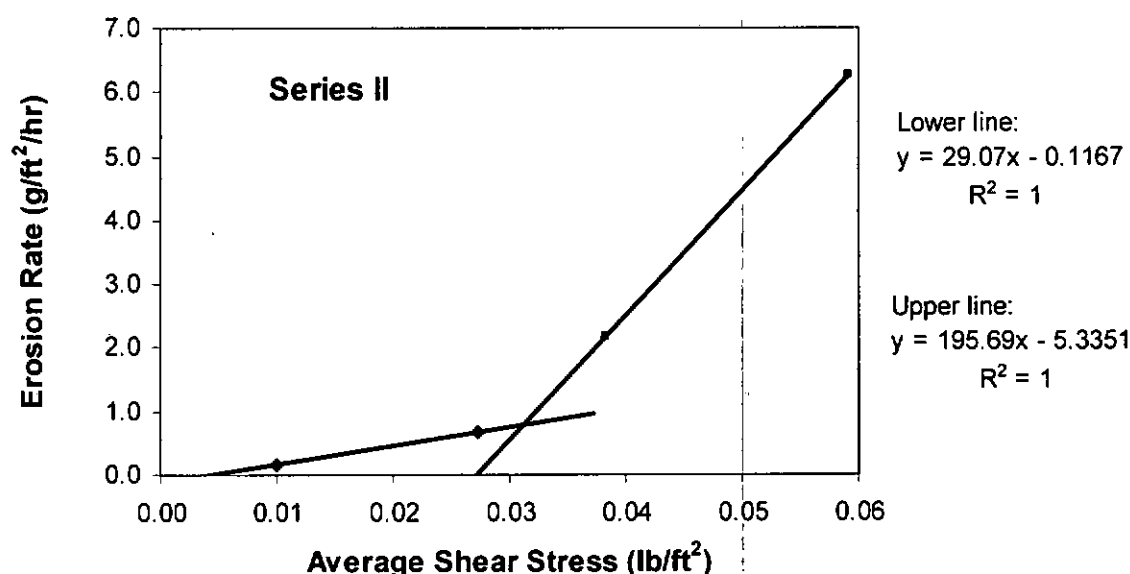


Figure 3-7. Plot of Series II rate of erosion versus average shear stress (data from Partheniades 1965).

For the sake of completeness, the results for Series III tests are plotted in Figure 3-8. There is much data scatter in the original results and a linear fit does not represent the data very well ($R^2 = 0.03$). An improvement to the fit is obtained if the erosion rates are averaged over specified shear stress levels. No discernable "break" is apparent due to the scatter in the data. The results are also presented in Table 3-3.

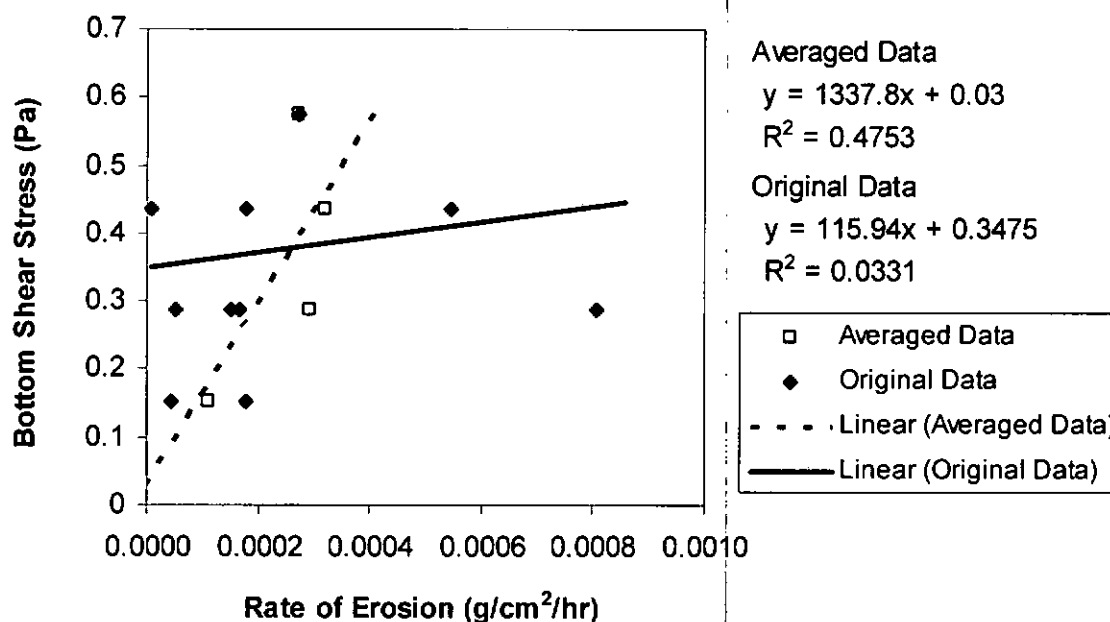


Figure 3-8. Plot of Series III data from Partheniades (1965) for bottom shear stress versus rate of erosion. Original data is shown by solid dark blue diamonds and average erosion rates at each bottom shear stress level are depicted by open violet squares. The above figure does not represent a piecewise linear fit, but two separate linear fits.

Table 3-3. Summary of shear strengths from present analysis and Partheniades (1965).

Series	Bed surface shear strength, τ_{so}		Characteristic shear strength, τ_{sc}	
	Present analysis [Pa]	Partheniades 1965 [Pa]	Present analysis [Pa]	Partheniades 1965 [Pa]
I	0.0234		0.4421	0.4788
II	0.1922		1.4996	1.3405
III – original data	0.3475			
III – averaged data	0.0300			
average	0.1078 ^a	0.057 ^b	0.9708 ^a	0.9097 ^a

Notes: ^a Consists of Series I and II data only.

^b Partheniades' average includes all three series.

3.3 Operational Critical Shear Stress

Another definition for shear strength is given by Villaret and Paulic (Teeter 1987, App. B). It is the “operational” or “design” critical shear stress for erosion and is designated τ_c . It is determined by extending the upper line, if there is one, of a rate of erosion ε or concentration $C(t)$ versus bed shear strength plot to the ordinate = 0 axis (see Figure 3-9). If there is no

piecewise linear fit, e.g., insufficient data, data scatter, author's preference, etc., then the operational shear strength is the shear stress value at $y = 0$ of a line fit through all the data.

Many investigators simply ignore or are unable to determine Zone 1 behavior and simply report τ_c or τ_{sc} . As Parthenaides and Paaswell (1970, pg. 761) remark:

Most of the summarized work had the disadvantage of an arbitrary and subjective criterion for failure. In most cases, this criterion corresponded to a stage of very rapid scouring, i.e., a state of failure.

It can be seen that the value of τ_c is intermediate to τ_{so} and τ_{sc} , e.g., $\tau_{so} < \tau_c < \tau_{sc}$.

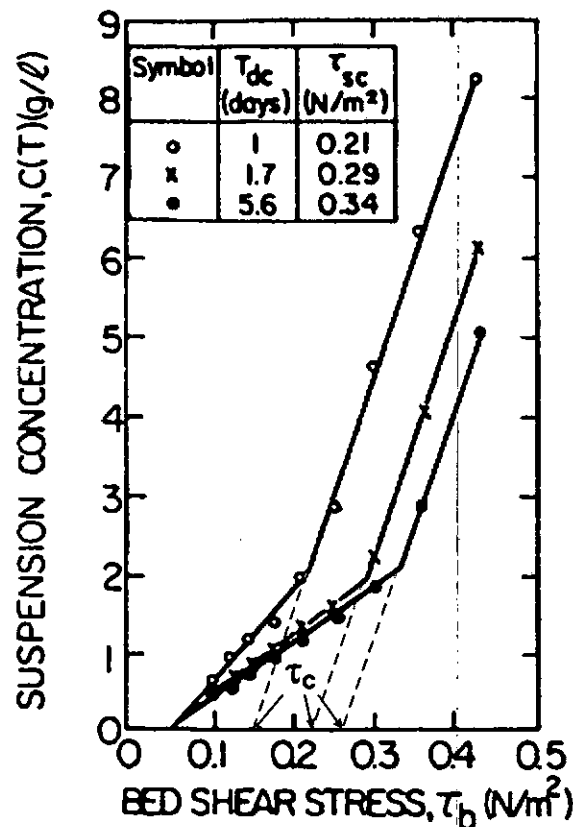


Figure 3-9. Concentration $C(t)$ at the end of each time step versus bed shear stress, τ_b , for a kaolinite sediment bed in salt water. Illustrated is the definition of the operational or design shear strength of the bed, τ_c . (Modified from Parchure and Mehta 1985, Figure 6)

3.4 Recommendation for the Waste Shear Strength Value

In light of the above discussion, it is felt that the values τ_c or τ_{sc} are more representative of the shear strength of the waste than τ_{so} . The value τ_{so} is a surface phenomenon and would represent a flow moving across the top of a sediment bed in a flume experiment or marine environment

(Figure 3-10a). However, in an intrusion event, drilling would cut down through the mass of degraded waste (Figure 3-10b). The drilling mud would flow up the borehole in a direction perpendicular to the upper surface. The strength of the mass of the degraded waste is better represented by τ_c or τ_{sc} , the strength values of the entire mass. These represent the minimum shear strength of the material in the bed. Theoretically, due to consolidation, the lower layers of the bed of degraded waste reach a maximum value of τ_{sm} , which is very nearly a constant. However, values of τ_{sm} seem to be rarely reported and it is probable that this idea is more applicable to experimental work rather than field conditions where much more pressure and much longer times are available. Therefore, use of τ_c or τ_{sc} as the shear strength of the waste is conservative.

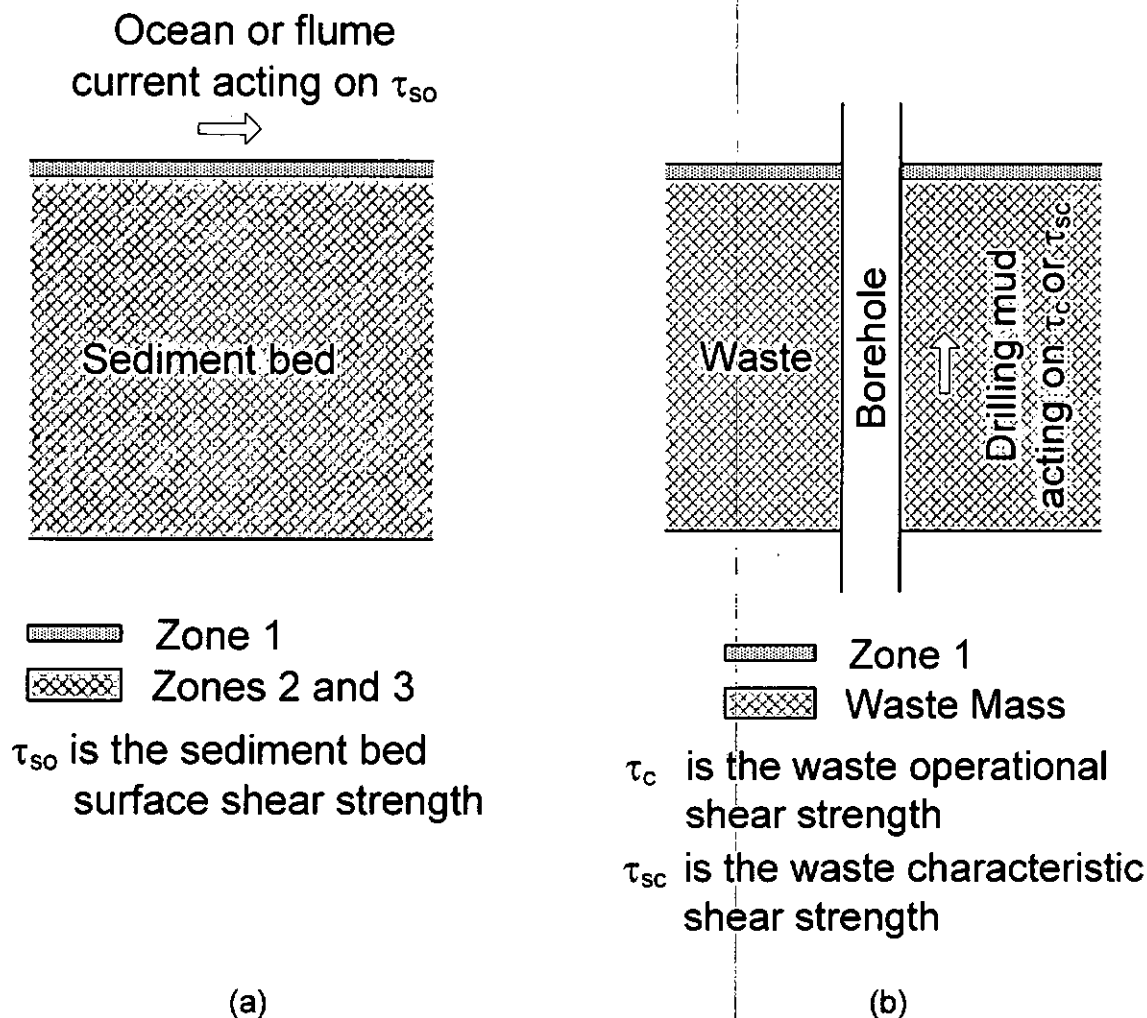


Figure 3-10. Schematic of various shear strengths and the direction of the currents acting on them: (a) flume experiment and (b) WIPP repository.

This idea of using the bed characteristic shear strength was substantiated in an e-mail from J. Buffington to C. Herrick (Buffington 2007). Dr. Buffington was the first author of a paper which

cataloged more than 80 years of incipient motion data (Buffington and Montgomery 1997). In that e-mail Dr. Buffington states:

However, I'm not sure how useful these data will be to your problem. Seems like you are interested in the shear strength, which is not quite the same as incipient motion from a streambed.

Incipient motion is a term for the beginning of surface erosion, which occurs at τ_{so} . Shear strength in this context refers to the characteristic shear strength of the bed.

4 Review of Analysis Based on Expert Panel's Particle Distribution

In this approach the critical shear stress of the waste (TAUFAIL) is hypothesized to depend on the waste particle size. A waste particle size distribution was constrained based on an expert panel elicitation mandated by the Environmental Protection Agency (EPA) for WIPP PAVT. The waste particle diameter was identified by the EPA as lacking supporting evidence (Trovato 1997a) and requiring derivation through expert judgment in Trovato (1997b). According to the second letter (Trovato 1997b):

The one parameter remaining (#2, ID# 3246, Material BLOWOUT, Parameter PARTDIA, waste particle diameter in Cuttings Model for direct brine release) is considered "sensitive" but the value for that parameter is not supported by data. Therefore, the parameter value must be derived through "expert judgment" in accordance with EPA's WIPP Compliance Criteria at 40 C.F.R. §194.26 (expert judgment) and 40 C.F.R. §194.22(a)(2)(v) (quality assurance procedures for the implementation of expert judgment elicitation).

Furthermore in Enclosure 2 of that same letter it says:

ID#	Material ID	Parameter ID	Description	Parameter to be Used in Verification Test
2254	BOREHOLE	TAUFAIL	Waste Shear Strength	Dependent on Results of Particle Size Distribution Expert Elicitation. ¹

¹ The values for this parameter are dependent on the results of the expert elicitation for the particle size distribution. Once the particle size is established via the expert elicitation, TAUFAIL should be calculated based on Shields Parameter (see, for example, Simon, D.B. and Senturk, F., 1992, *Sediment Transport Technology: Water and Sediment Dynamics*) as a function of particle diameter.

Based on an analysis of the expert elicitation results (CTAC 1997), the lower limit of the mean particle size of WIPP waste was estimated to be 1 mm, while the upper limit was determined to be either 10 cm assuming no cementation or approaching room size when cementation occurs (Wang 1997). This range was determined by converting the expert elicitation panel's particle size distribution to a volume fraction basis and considering complete waste degradation. For the purposes of calculating the critical shear stress in the waste, Wang and Larson (1997) assumed a minimum mean particle density of 2.5 g/cm³. The Department of Energy's (DOE) approach was

to use the Shield's parameter following the method in Simon and Senturk (1992) as suggested by the EPA (Trovato 1997b) and as outlined in a facsimile to DOE by T. Peake (1997).

The Shields parameter is a measure of threshold condition between erosion and sedimentation of a single particle (Julien 1998). This condition is usually referred to as incipient motion, a term for the beginning of surface erosion. Fluid flow around sediment particles exerts forces that tend to initiate particle motion (τ_{so}). The resisting force of non-cohesive material relates to particle weight. Threshold conditions occur when the hydrodynamic moment of forces acting on a single particle balances the resisting moment of force. The Shields diagram remains the most widely used criterion for incipient motion of sediment tests (Coa et al. 2006). The critical value of the Shield's parameter, ψ_c , corresponding to the beginning of motion depends on whether laminar or turbulent flow conditions prevail around the particle. The mean particle sizes averaged on volume fractions were used to calculate the parameter TAUFAIL since the Shields parameter is a dimensionless measure of τ_{so} .

Wang and Larson's Table 2 is reproduced below as Table 4-1. The range of mean particle diameters of interest is 1 mm to 10 cm (Wang 1997), which yields values for the critical shear stress of WIPP waste as 0.64 Pa for 1 mm particles and 76.52 Pa for 10 cm particles. The DOE chose not to use the lower limit for TAUFAIL and recommended using the CCA value of 0.05 Pa to be conservative and as directed by Kruger (1997). The EPA accepted the lower value of 0.05 Pa "for conservatism" (EPA 1998).

The particle size distribution as determined by the Expert Panel Elicitation fills one of the gaps mentioned by the Conceptual Model Peer Review (DOE 1996, Appendix Peer, Peer 1, Conceptual Models Peer Review Report (July 1996)) in that it provides knowledge of the future state of the waste.

Table 4-1. Critical shear stress of WIPP waste calculated as a function of waste mean particle diameter (Wang and Larson 1997, Table 2).

Particle diameter d_g (m)	Grain scale Re	Shields parameter ψ_c	TAUFAIL (Pa)
1.00E-04	17	0.033	0.04
1.00E-03	170	0.05	0.64
5.00E-03	850	0.06	3.83
1.00E-02	1700	0.06	7.65
2.00E-02	3400	0.06	15.30
5.00E-02	8500	0.06	38.26
6.00E-02	10200	0.06	45.91
8.00E-02	13600	0.06	61.21
1.00E-01	17000	0.06	76.52
2.00E-01	34000	0.06	153.04

5 Tests on Surrogate Waste Materials

Jepsen et al. (1998) performed erosional shear testing on partially and highly degraded surrogate waste samples developed by Hansen et al. (1997). The degraded waste material properties were summarized for the spillings model review panel by Hansen et al (2003). The material was developed in a logical, systematic manner based on consideration of the anticipated future state of the waste considering inventory, evolution of the underground environment, and experimental results.

Conceptualization of the underground, based on waste disposal configurations and analyses of the rock mechanics response, suggested that the most likely future state of the waste materials includes crushing, compaction, and entombment by the surrounding salt. The waste inventory is comprised of massive steel components including standard 55-gallon drums, standard waste boxes, thick steel pipe overpacks, and supercompacted waste "pucks" stored in overpacks. The bulky nature of the compressed inventory makes freeing and transporting of radionuclides extremely difficult. In the most extreme cases, however, the expected processes of iron corrosion and microbial activity can result in predictions of extensive degradation. This end state represents a bounding condition for the waste, which provides a means to quantify the lowest strength conditions of the future state of the waste, and is appropriate for representing the lower bound strength of degraded waste from uncompacted drums and standard waste boxes. Other, denser, waste forms such as pipe overpacks and supercompacted waste packages would be expected to degrade and corrode to a much lesser extent, and therefore will have material characteristics which are much less conservative than those assumed for standard wastes.

Therefore, Hansen et al. (1997, Appendix A) developed their model material from the estimated inventory of standard waste drums. The surrogate waste comprised a mixture of raw materials including iron, glass, cellulose, rubber, plastic, solidification cements, soil, and WIPP salt. They considered degradation of each waste constituent. Subsurface processes leading to extreme degradation are based on several contributing conditions including ample brine availability, extensive microbial activity, corrosion, and the absence of cementation and salt encapsulation effects. The authors asserted that the degraded waste material properties represented the lowest plausible realm of the future waste state because no strengthening processes were included such as compaction, cementation, mineral precipitation, more durable packaging and compressed waste, and less corrosion. It is believed that the samples used by Jepsen et al. (1998) represent an unobtainable degraded state of the waste and are thus far weaker than any possible future state, including any percentage changes that may occur in the waste inventory (Hansen et al 1997, 2003; Hansen 2005). It is therefore believed that this represents a very conservative approach.

Jepsen et al. (1998) performed their tests using an apparatus (Sedflume) developed at the University of California-Santa Barbara. The flume is 120 cm long by 10 cm wide by 2 cm high rectangular duct which is constructed of clear acrylic to allow sample-water interactions to be observed. Integrated into the end of the duct is the 10 cm wide by 15 cm long test section. During the test as the material erodes an operator continuously moves the sample upwards such that the sample-water interface remains level with the bottom of the flume. The erosion rate is recorded as the upward movement as a function of time.

Three types of waste materials were tested. The Chain of Custody (COC) records identifying the types of samples are found in RESPEC's laboratory notebook (Mellegard 1998).

1. Category I consists of five samples of 50% degraded (i.e., degradation of the iron-based inventory) surrogate material designated B1 thru B6.

B1 No COC found but there is a memo from RE/SPEC to UCSB dated 12/03/1997 describing the sample. This sample was not used as it would not fit into the sample holder.

B2 & B3 COC Ref. No. 325/1-98/45, RE/SPEC to UCSB dated 01/23/1998

B4, B5, & B6 COC Ref. No. 325/2-98/34, RE/SPEC to UCSB dated 02/12/1998

2. Category II consists of three samples of 100% degraded surrogate material designated B7 thru B9.

B7, B8, & B9 COC Ref. No. 325/5-98/28, RE/SPEC to UCSB dated 05/15/1998

3. Category III consists of five magnesium oxide (MgO) bricks designated B11 thru B15.

B10, B11, & B12 COC Ref. No. 325/5-98/37, RE/SPEC to UCSB dated 05/19/1998

B13, B14, & B15 COC Ref. No. 325/6-98/5, RE/SPEC to UCSB dated 06/29/1998

Notes:

- 1) Sample B10 description is 100% MgO – Air Dried. Sample B10 was received in a damaged state and was not tested.
- 2) Samples B11 thru B15 descriptions are 100% MgO – Brine Saturated.

The Jepsen et al. (1998) data of average erosion rates for the calculated shear stresses for the samples tested are given in Table 5-1.

The measurement of critical shear stress for erosion is described in Jepsen et al. (1998, pg. 7) as follows:

A critical shear stress can be quantitatively defined as the shear stress at which a very small, but accurately measurable, rate of erosion occurs. In the present study, this rate of erosion was chosen to be 10^{-4} cm/sec; this represents 1 mm of erosion in approximately 15 minutes. Since it would be difficult to measure all critical shear stresses at exactly 10^{-4} cm/sec, erosion rates were generally measured above and below 10^{-4} cm/sec at shear stress which differ by a factor of two. The critical shear stress was then linearly interpolated to an erosion rate of 10^{-4} cm/sec. This gave results with a 20% accuracy for the critical shear stress. Some of the samples could not be eroded at rates greater than 10^{-4} cm/sec within the range of shear stresses possible. For these samples, the test was run at a particular shear stress for several hours in order to obtain a measurable amount of erosion.

The shear stress was calculated using Prandtl's Universal Law of Friction for a pipe with a smooth wall, namely:

$$\frac{1}{\sqrt{\lambda}} = 2.0 \log \left[\frac{UD\sqrt{\lambda}}{\nu} \right] - 0.8 \quad (5-1)$$

where λ is the friction factor, U is the mean flow speed (cm/sec), D is the hydraulic radius (cm), and ν is the kinematic viscosity (cm²/sec).

The kinematic viscosity, ν , is defined as η/ρ , where η is the dynamic viscosity (g/(cm sec)) and ρ is the mass density (g/cm³).

For a pipe with a rectangular cross section, as in Sedflume, the hydraulic diameter is given as

$$D = \frac{2hw}{h + w} \quad (5-2)$$

where h is the duct height (cm) and w is the duct width (cm).

The friction factor is defined as

$$\lambda = \frac{8\tau}{\rho U^2} \quad (5-3)$$

where λ is the friction factor, τ is the wall shear stress, ρ is the density of water, and U is the mean flow speed.

Inserting Eqs. 5-2 and 5-3 into 5-1 the wall shear stress (τ) is given as an implicit function of the mean flow speed (U).

Table 5-1. Average erosion rates (cm/sec) for each shear stress (dyne/cm²) (Jepsen et al. 1998, Table 1)

Sample	Shear Stress (dynes/cm ²) ^a												
	2	3	4	6	8	12	14	16	20	24	32	40	64
B1 ^b													
B2						5.5E-05		8.5E-05	1.7E-04	1.4E-03			
B3										2.0E-04	1.7E-03	2.2E-03	
B4						1.4E-04		2.3E-03	8.3E-03				
B5 ^c					1.7E-04								
B6 ^d							8.3E-5	8.3E-05					
B7	5.6E-05	3.3E-04	6.6E-04	5.0E-03	7.6E-03								
B8		1.0E-04	3.1E-04	8.3E-04	1.5E-03	4.4E-03							
B9		5.6E-05	2.1E-04	5.7E-04	1.8E-03								
B10 ^e													
B11													2.6E-05
B12													4.6E-06
B13S ^f													2.3E-05
B13F ^f													1.8E-05
B14S ^f								2.8E-05			3.7E-05		4.3E-05
B14F ^f								5.9E-05			5.5E-05		4.0E-05
B15S ^f			2.0E-04			4.3E-03							
B15F ^f			1.7E-04			3.3E-03							

Notes: ^a One pascal is equal to 1/10th of a dyne/cm²

^b Sample B1 was too large to fit in tube.

^c Only one data point. At the next shear stress level the "flow meter's paddle wheel was destroyed from recirculating debris caught in the apparatus" (Jepsen et al. 1998, p. 11).

^d Values differ from those reported in the original table. Listed values were changed based on information given in text: "A test was run for a shear stress of 14 dyne/cm². In ten minutes, 0.5 mm of material was eroded. This is very close to an erosion rate of 10⁻⁴ cm/s which is defined as the erosion rate for critical shear stress. The erosion test was repeated for 16 dyne/cm² and showed similar erosion rates with depth." (Jepsen et al. 1998, p. 12).

^e Sample B10 was received destroyed.

^f S means tested in salt water conditions and F means tested under fresh water conditions.

Table 5-2 contains the values of the critical shear strengths as obtained using the methodology described by Jepsen et al., i.e., the shear stress evaluated at an erosion rate of 10^{-4} cm/sec.

Table 5-2. Critical shear stresses for each sample as determined by Jepsen et al. (1998, Table 2)

Sample	Critical Shear Stress	
	dyne/cm ²	Pa
Category I		
B1	—	—
B2	16.7	1.67
B3	22.0	2.20
B4	10.6	1.06
B5	7.2	0.72
B6	14.0	1.40
Category II		
B7	2.2	0.22
B8	3.0	0.30
B9	3.4	0.34
Category III		
B10	—	—
B11	>64	>6.4
B12	>64	>6.4
B13	>64	>6.4
B14	>64	>6.4
B15	2.0	0.20

As discussed in Section 3.1, there are two types of erosion. The first is “surface erosion” in which erosion takes place by the removal of individual particles and/or small clusters (flocs) when hydrodynamic forces overcome the bonds formed between particles (Parchure and Mehta 1985, Partheniades and Paaswell 1970). Surface erosion takes place in Zone 1 which is on the order of millimeters or less. The bed surface shear strength (τ_{so}) can be quantitatively defined by extrapolating the first of the two linear segments that characterize an erosion rate versus shear stress plot to an erosion rate of zero.

The second is “bed erosion” (Parchure and Mehta 1985) or “mass erosion” (Partheniades and Paaswell 1970) in which erosion takes place by the removal of relatively large pieces of soil. Bed erosion is initiated when flow induced forces on the bed causes stresses within the sediment to exceed the shear strength along localized planes. It is usually defined as the break in the erosion rate versus shear stress plot above which erosion rates increase more rapidly with shear stress than below the critical value. The onset of bed erosion is demarked by the bed’s characteristic shear strength (τ_{sc}). This point can be quantitatively determined by fitting two piecewise linear curves to the data and evaluating the intersection.

As also mentioned in Section 3.3, there is a third shear strength value that is used to characterize the strength of the bed, that is, the “operational shear strength” (τ_c). It is obtained by fitting a single line through the data after which the erosion rate increases at a much faster rate. The intercept of that line with the shear stress axis defines the operational shear strength. For samples in which the data do not indicate an increase in erosion rate, a linear fit was used for all the data. This single line fit through all the data extended back to zero erosion rate was also called τ_c .

Table 5-3 gives the values of τ_{so} , τ_{sc} , and τ_c based on curve fitting the results from Jepsen et al.’s (1998) testing of surrogate waste materials. The data for Category III waste (MgO bricks) are not included since they are not considered waste. Plots of each test are shown in Figure 5-1 through Figure 5-9.

Table 5-3. Summary of shear strengths from present analysis and Jepsen et al (1998).

Sample	Present Analysis Piecewise Linear Fit		Present Analysis Operational shear strength (τ_c) [Pa]	Jepsen et al. (1998) reported shear strength values [Pa]
	Bed surface shear strength (τ_{so}) [Pa]	Bed characteristic shear strength (τ_{sc}) [Pa]		
Category I				
B2	0.47	1.98	1.94	1.67
B3 ^a	—	—	2.11	2.20
B4 ^a	—	—	1.25	1.06
B5 ^{b, d}	—	—	0.80	0.72
B6 ^{c, d}	—	—	1.40	1.40
average	0.47	1.98	1.50	1.41
Category II				
B7	0.18	0.38	0.35	0.22
B8	0.27	0.76	0.59	0.30
B9	0.26	0.59	0.51	0.34
average	0.24	0.58	0.48	0.29

Notes: ^a Insufficient data for piecewise linear curve fit.

^b Test series incomplete and stopped at one shear stress level because flow meter was destroyed by debris at the next level. Keeping data point adds conservatism.

^c Like Jepsen et al (1998), present analysis uses lowest value reported for shear stress causing erosion. See Note d of Table 5-1.

^d Insufficient data for piecewise linear or linear curve fit.

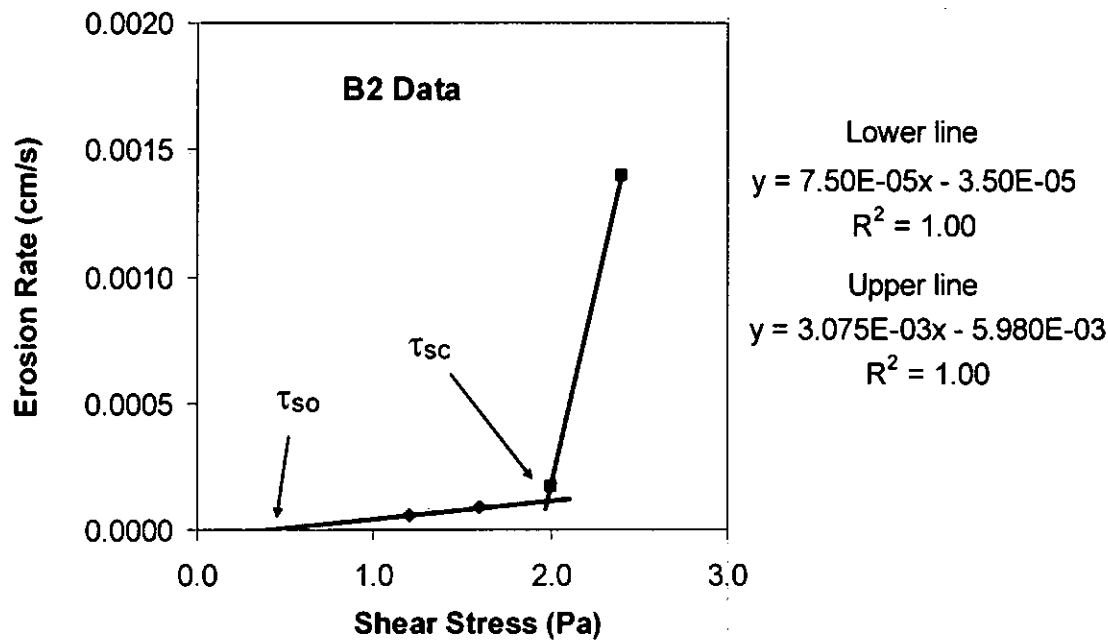


Figure 5-1. Piecewise linear fit to data from Sample B2 (Jepsen et al. 1998) to obtain bed surface shear strength (τ_{so}) and bed characteristic shear strength (τ_{sc}).

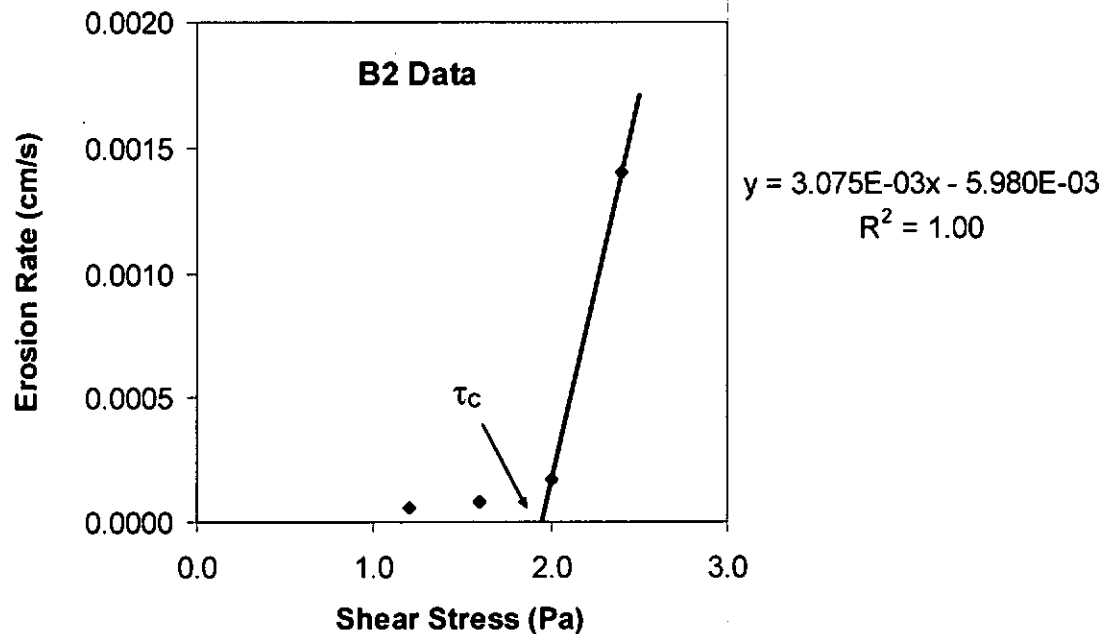


Figure 5-2. Linear fit to data of Sample B2 (Jepsen et al. 1998) after which the erosion rate increases sharply to obtain the operational shear strength τ_c .

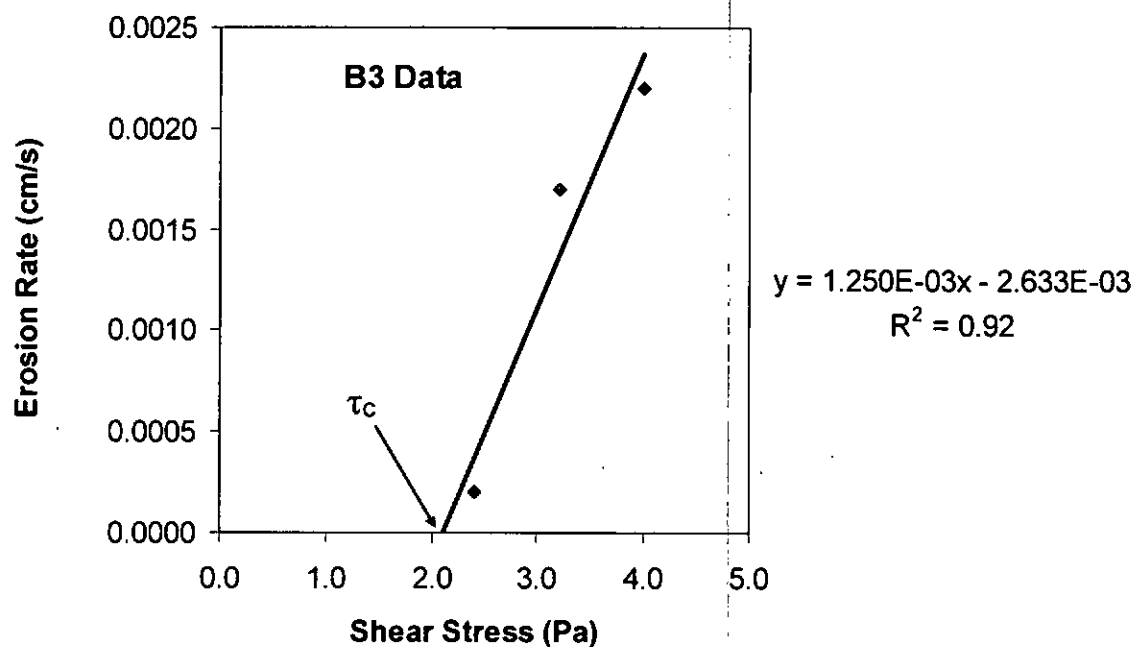


Figure 5-3. Linear fit to all the data of Sample B3 (Jepsen et al. 1998) to obtain the operational shear strength τ_c .

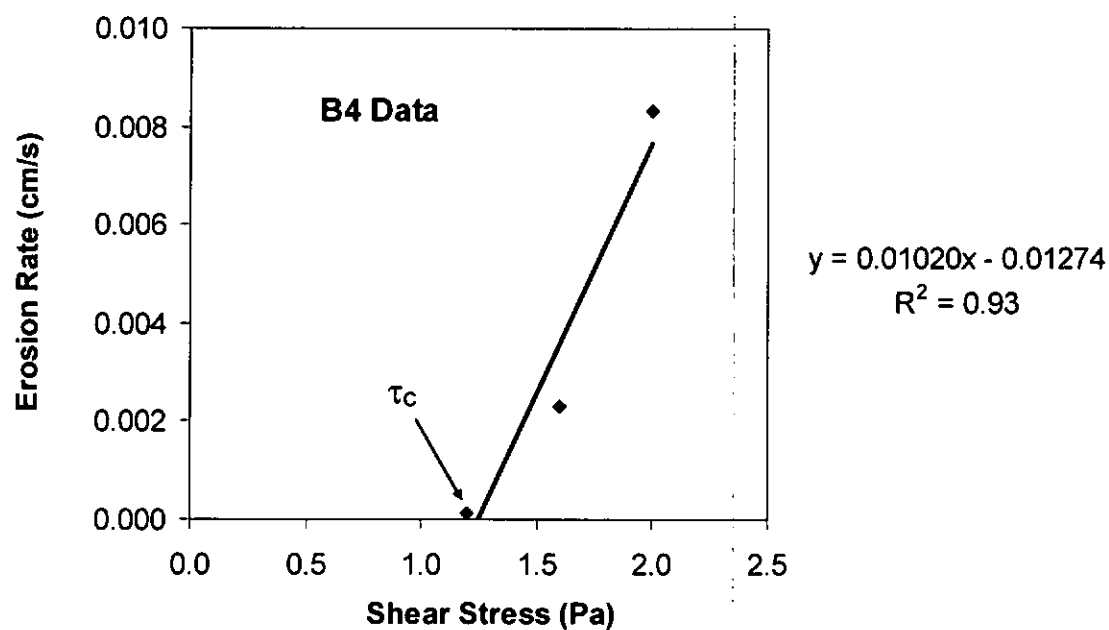


Figure 5-4. Linear fit to all the data of Sample B4 (Jepsen et al. 1998) to obtain the operational shear strength τ_c .

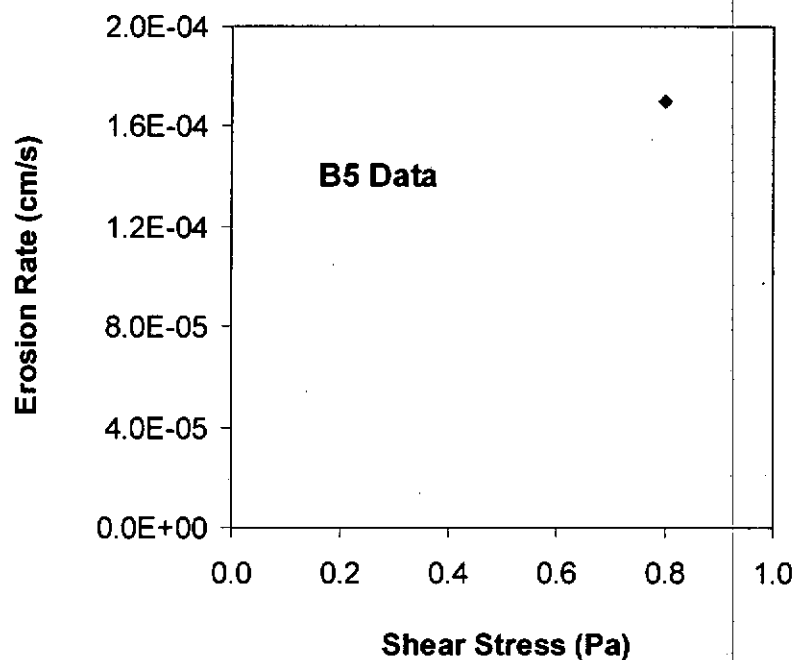


Figure 5-5. Plot of data from Sample B5 (Jepsen et al. 1998). Test series was stopped at one shear stress level because flow meter was destroyed by debris at the next shear stress level.

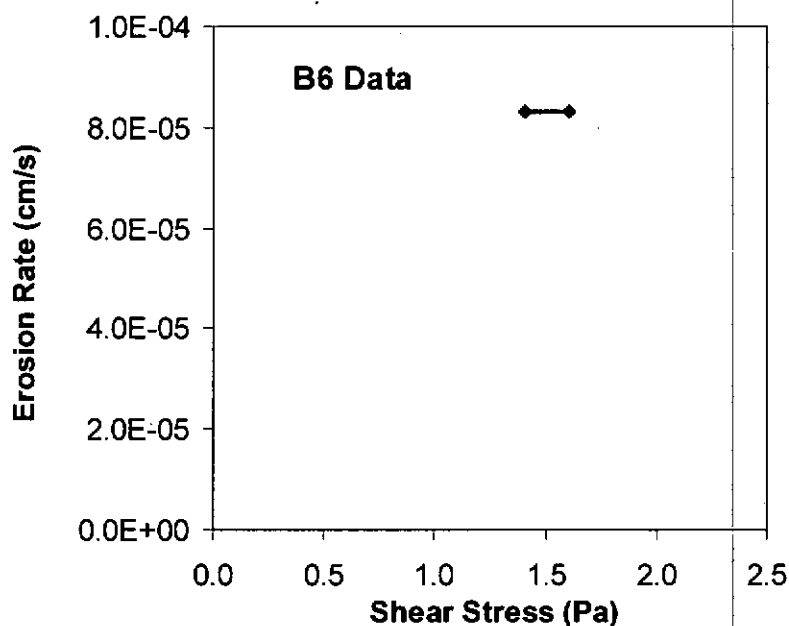


Figure 5-6. Plot of data from Sample B6 (Jepsen et al. 1998). Like Jepsen et al (1998), present analysis uses lowest value reported for shear stress causing erosion. See Note d of Table 5-1.

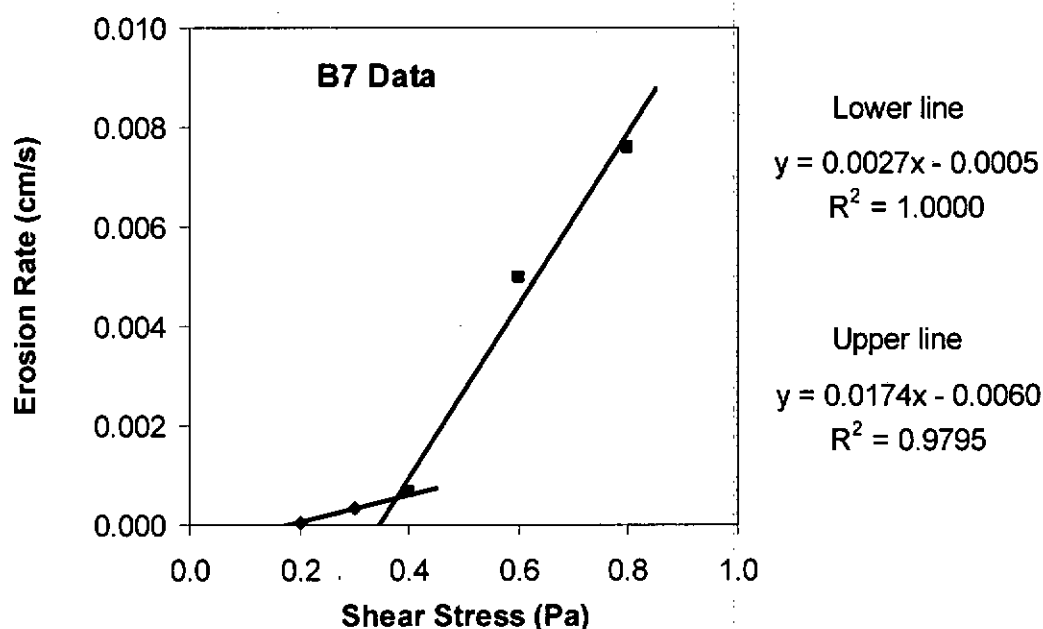


Figure 5-7. Piecewise linear fit to data from Sample B7 (Jepsen et al. 1998) used to obtain bed surface shear strength (τ_{so}), operational shear strength (τ_c), bed characteristic shear strength (τ_{sc}).

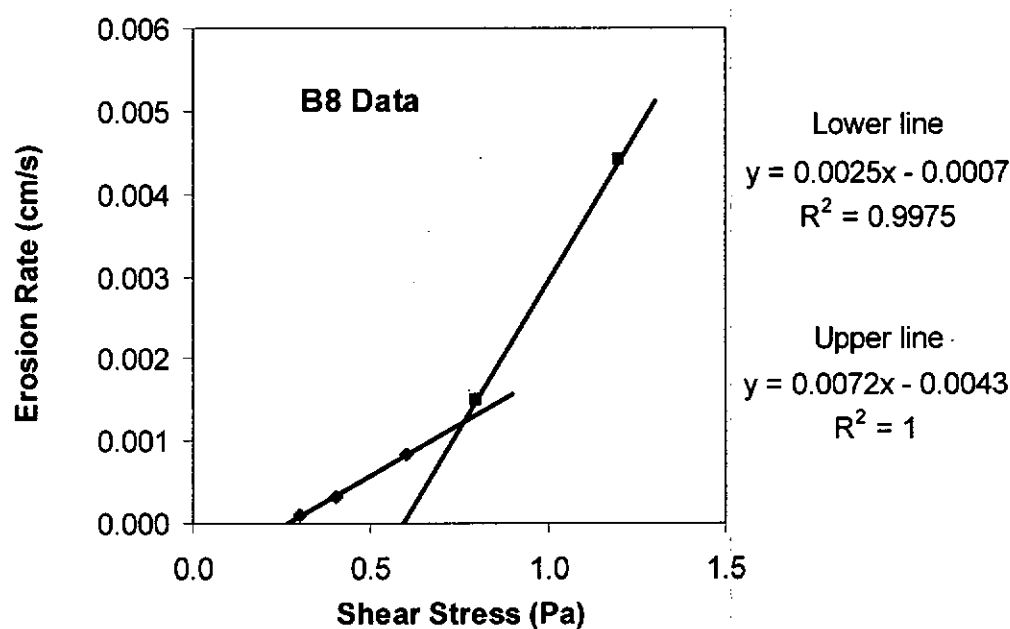


Figure 5-8. Piecewise linear fit to data from Sample B8 (Jepsen et al. 1998) used to obtain bed surface shear strength (τ_{so}), operational shear strength (τ_c), bed characteristic shear strength (τ_{sc}).

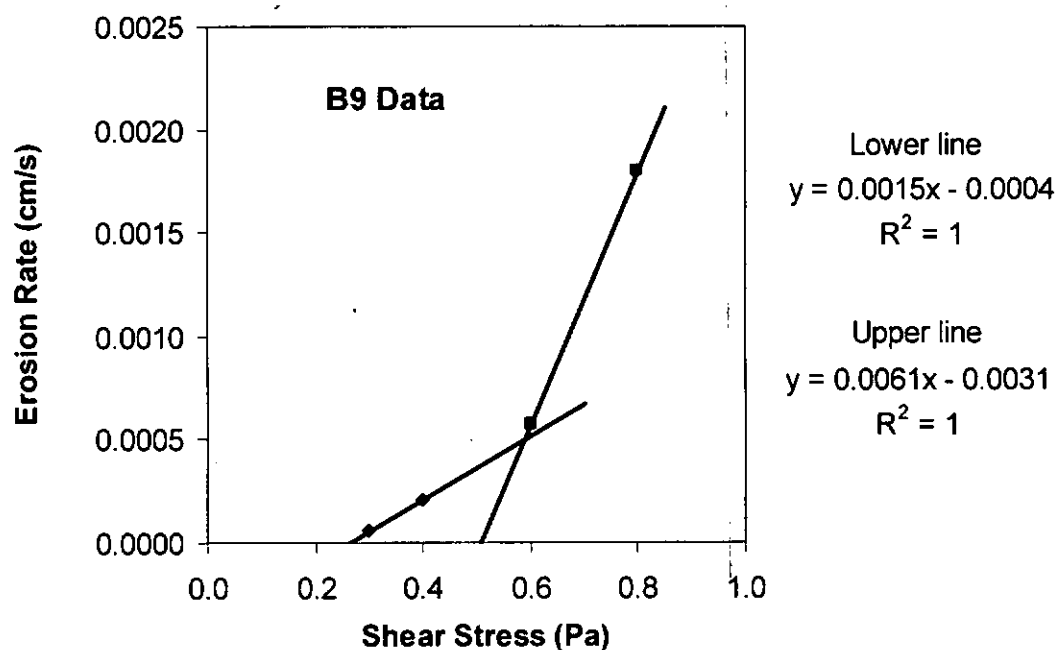


Figure 5-9. Piecewise linear fit to data from Sample B9 (Jepsen et al. 1998) used to obtain bed surface shear strength (τ_{so}), operational shear strength (τ_c), bed characteristic shear strength (τ_{sc}).

Hansen et al. (2003) used the experimental results for the 50% degraded surrogate waste material to obtain the parameters used in the DRSPALL code. The reason was that for most performance assessment calculations that amount of initial iron inventory or more remains. Following Hansen et al.'s lead, the amount of iron remaining under the undisturbed scenario for the present re-certification effort (CRA-2009) is shown in Figure 5-10. In addition, the worst case scenario (E1@350 years) is shown in Figure 5-11. Both plots show that for the vast majority of vectors the amount of iron remaining is more than 50%, and in no case is there less than 30%. Therefore, in accord with Hansen et al. (2003), we recommend accepting the experimental results for the 50% degraded samples. To be conservative, we also recommend using the value of τ_c as it fits the majority of the data the best. Using this approach, the shear strength of the surrogate materials is 1.50 Pa on average.

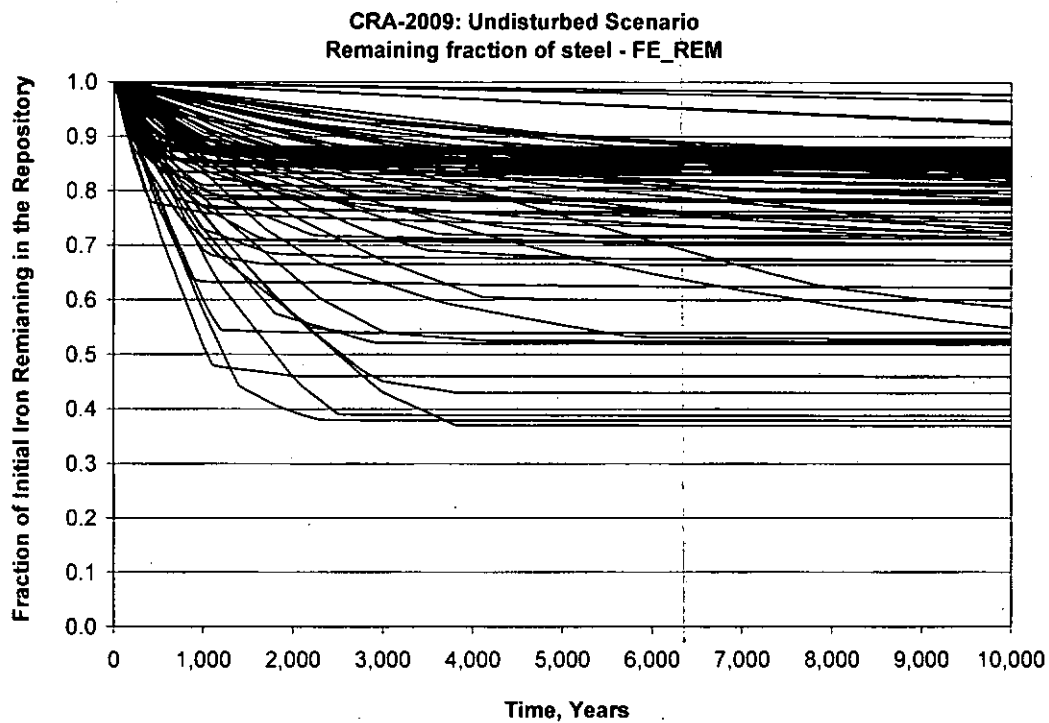


Figure 5-10. Iron remaining in WIPP from present recertification calculations for the undisturbed scenario.

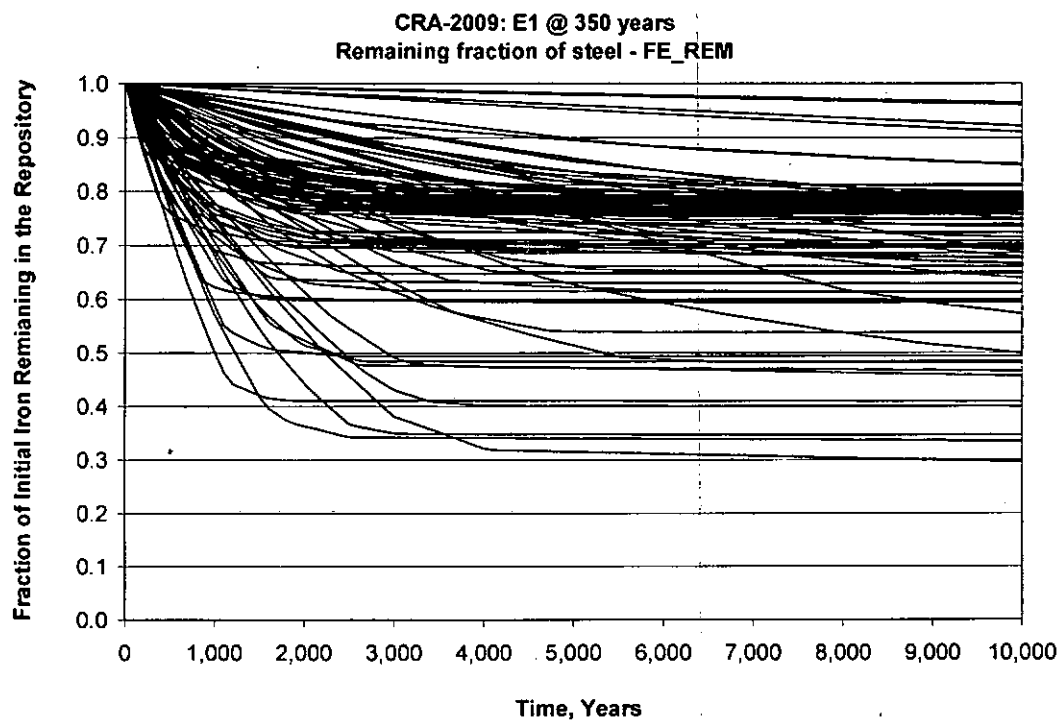


Figure 5-11. Iron remaining in WIPP from present recertification calculations for the E1 scenario at 350 years as the worst case.

Information Only

6 Waste Permeability and the Possibility of Stuck Pipe / Gas Erosion

Stuck pipe and gas erosion are postulated to occur if the waste permeability is less than 10^{-16} m^2 and if certain gas pressure conditions are met: if the gas pressure exceeds 8 MPa, gas erosion can occur, and if it exceeds 10 MPa, stuck pipe can occur (Butcher 1995). In the CCA, the DOE assigned a value of $1.7 \times 10^{-13} \text{ m}^2$ for the permeability of the waste based on the permeabilities of the waste components. Since this value is greater than that which would cause gas erosion or stuck pipe to occur, the DOE did not model these processes. The results of the CCA showed that total releases are dominated by short term releases associated with inadvertent drilling intrusions into the waste and attention was shifted to examining these by Hansen et al. (1997).

Hansen et al. (1997) developed surrogate materials to investigate models for estimating solids volumes that may be released during spalling events. As discussed in Section 5 the materials they developed represent the anticipated future state of the waste considering inventory and the underground environment. The surrogate waste comprised a mixture of raw materials including iron, glass, cellulose, rubber, plastic, solidification cements, soil, and WIPP salt. No strengthening processes were included in the material mixtures such as compaction, cementation, mineral precipitation, more durable packaging and compressed waste, and less corrosion. Therefore it is believed that the samples represent an unobtainable degraded state and are thus far weaker than any possible future state of the waste (Hansen et al 1997, 2003; Hansen 2005).

Hansen et al. (1997) measured the permeability of two surrogate waste samples (S14 and S24). The measured permeabilities were 5.3×10^{-15} and $2.1 \times 10^{-15} \text{ m}^2$, respectively, which are two orders of magnitude less than the value used in the CCA. Consider S24, which was designed to simulate 50% corrosion and degradation of the organics, for example. The porosity of this sample was not measured, however the porosity of similar samples using the same recipe have an average porosity of 0.209. This is approximately the same as the porosity of the waste at 10,000 years considering only salt creep with no gas generation ($\phi = 0.205$, Herrick et al. 2007). The gas generation factor that produces gas pressures of 8 MPa is $f = 0.2$. The porosity in the waste after 10,000 years in this case, considering both loading and secondary compression, the most conservative case as it leads to the most compaction, is 0.414 (Figure 6-1).

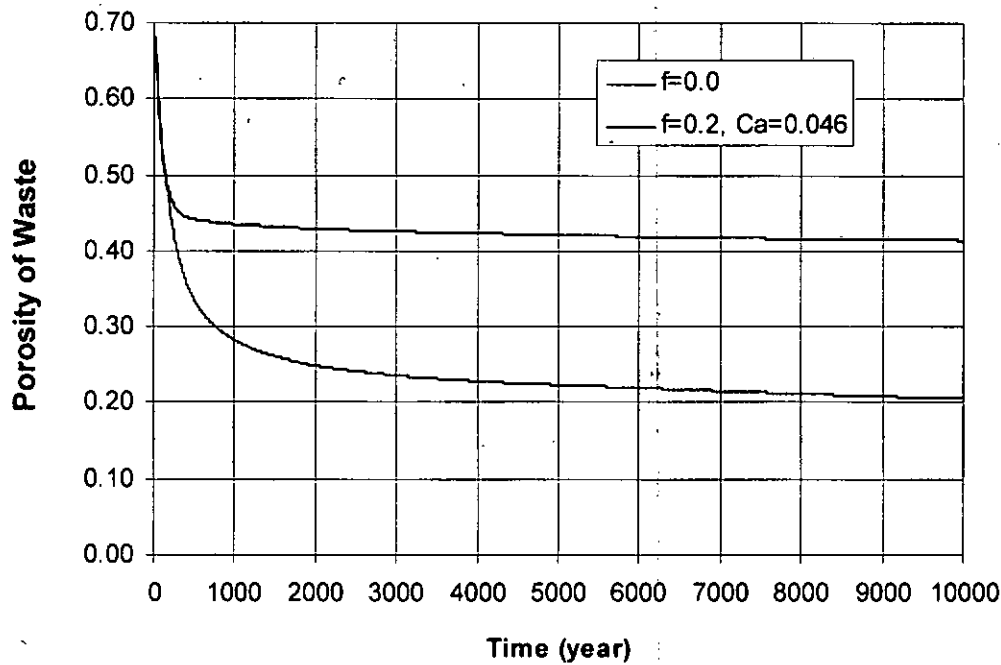


Figure 6-1. Porosity of waste as a function of time for the cases of $f = 0.0$ with only salt creep considered and $f = 0.2$ considering loading and secondary compression (Herrick et al. 2007).

At the $f = 0.2$ condition, the permeability of the waste can be estimated from the Kozeny-Carmen equation (Das 2006):

$$\frac{k_1}{k_2} = \frac{\left(\frac{e_1^3}{1+e_1} \right)}{\left(\frac{e_2^3}{1+e_2} \right)} \quad (6-1)$$

where k_1 is the known hydraulic conductivity for the condition $f = 0.0$, k_2 is the hydraulic conductivity for the condition $f = 0.2$, e_1 is the void ratio for $f = 0.0$, and e_2 is the void ratio for $f = 0.2$. The ratio of hydraulic conductivities k_1/k_2 can also represent the ratio of permeabilities K_1/K_2 since the fluid properties are the same. Converting porosities to void ratios and invoking Eq 6-1, the permeability K_2 at $f = 0.2$ is estimated to be $3.0 \times 10^{-14} \text{ m}^2$. This is two orders of magnitude greater than the required permeability of 10^{-16} m^2 for either gas erosion or stuck pipe. A similar result would be obtained for sample S14. Permeabilities for higher gas generation factors will be even greater since the change in porosity due to compression is less.

Therefore, it does not appear to be possible to meet both the permeability and pressure requirements necessary for either stuck pipe or gas erosion. At the estimated permeabilities for waste undergoing both loading and secondary compression, blowout remains the only expected release mechanism.

7 Summary and Recommendation

7.1 Summary

This report has reexamined the lower limit of the waste shear strength as it is applied in the code CUTTINGS_S. The shear strength parameter used in WIPP PA is BOREHOLE : TAUFAIL. The lower limit of the range of values used for TAUFAIL is presently set at 0.05 Pa. It was based on the shear stress required to cause incipient motion in a San Francisco Bay mud (Partheniades and Paaswell 1970). This analysis has looked at this value from a number of different view points and found this value to be excessively low.

At the time of the CCA, it was recognized that the particle size of the degraded waste was unknown. The particle size is known to influence the ability of sediment to erode – the greater the particle size, the more resistant the sediment is to erosion. The EPA required the DOE to conduct an expert panel evaluation of the anticipated particle sizes based on the best available knowledge (Trovato 1997a, b). The EPA accepted the findings of the expert panel, and therefore accepted the objective of the elicitation: to provide knowledge of the future state of the waste. The DOE applied the results in a Shield's diagram to determine the shear strength for incipient motion, another term for the beginning of surface erosion, and obtained a range 0.64 to 77 Pa. However, only the upper bound was accepted. The lower bound was rejected in favor of the more conservative value based on San Francisco Bay mud (EPA 1998).

The report also examines the use of applying erosion test results to the waste. It was noted that the use of the values obtained for incipient motion are not the values that should be used for the waste. The value of shear strength for incipient motion, which is denoted by τ_{so} in this analysis, is a surface phenomenon that pertains only to the first few millimeters of the sediment bed. The flow direction that gives rise to this value is across the surface, which is why τ_{so} is often referred to as the bed surface shear strength. On the other hand, a drill penetrating the waste will drill in a direction that penetrates the depths of the waste. In this case, the erosion will be occurring on a more dense material within the waste mass which is more able to resist erosion. In erosion experiments, Partheniades (1965) and Parchure and Mehta (1985) noted that there is a specific bed shear stress beyond which erosion of the bed at depth takes place. They refer to this as the characteristic shear strength of the bed (τ_{sc}) as it represents the behavior of the bed material, not a few loose grains on the bed surface. Typical erosion test results can be well represented by two lines (a piecewise linear fit) where the intersection of the two lines represents τ_{sc} (see Figure 3-3). The characteristic shear strength of the bed is a minimum value for the bed mass as a whole. Deeper into the bed, the density increases and the ability of the bed to resist erosion continues to increase. In laboratory experiments, the bed seems to reach a maximum value. However, this maximum value is thought to be an experimental remnant rather than something found in the field.

Other erosion studies of San Francisco Bay mud by US Army Corp of Engineers (Teeter 1987) introduced the use of yet another shear strength measure which they called the operational shear strength. We use their notation and denote this value by τ_c . It is determined by extending the upper line, if there is one, of a rate of erosion ε or concentration $C(t)$ versus bed shear strength

plot to the ordinate = 0 axis (see Figure 3-9). If there is no piecewise linear fit, e.g., insufficient data, data scatter, or author's preference, then the operational shear strength is the shear stress value at $y = 0$ of a line fit through all the data. The operational shear strength is intermediate to the surface and characteristic shear strengths ($\tau_{so} < \tau_c < \tau_{sc}$).

The value of the shear strength proposed for the waste in this analysis should be represented by either the bed operational (τ_c) or characteristic shear strength (τ_{sc}) value, not the value of incipient motion of the surface (τ_{so}).

In this analysis we also present the results of erosion experiments performed on surrogate waste materials developed for the spillings model. This material was developed in a logical and systematic fashion based on the expected WIPP waste inventory and consistent with future repository conditions. The analyses of Jepsen et al (1998) and this analysis are given in Table 5-3. The 100% degraded waste was weaker than the 50% degraded, however in neither case was the value of τ_{so} , which we do not recommend using, less than 0.2 Pa. The best measure of the surrogate waste material shear strength is the operational shear strength. On average, as reported by Jepsen et al. (1998), $\tau_c = 1.41$ and 0.29 Pa for the 50% and 100% degraded wastes, respectively. Our analyses using the method developed by Parchure and Mehta (1985) yields values of 1.50 and 0.48 Pa, respectively.

A summary of the results of our different studies are given in Table 7-1.

Table 7-1. Compilation of results from various analyses conducted in this analysis.

	τ_{so} [Pa]	τ_{sc} [Pa]	τ_c [Pa]
SF Bay mud ^a			
Partheniades (1965)	0.057	0.910	
Present analysis	0.108	0.971	
Expert elicitation ^b	0.64		
Surrogate material 50% degraded ^c			
Jepsen et al (1998)			1.41
Present analysis	0.47	1.98	1.50
Surrogate material 100% degraded ^c			
Jepsen et al (1998)			0.29
Present analysis	0.24	0.58	0.48

Notes: ^a See Table 3-3.

^b See Table 4-1.

^c See Table 5-3.

7.2 Recommendation

The analog model for the waste has been erosion of San Francisco Bay mud in spite of an expert panel providing what was believed to be knowledge of the future state of the waste.

For our recommendation we incorporate results which are considered representative of the waste as it is most likely to be encountered by a drilling intrusion, namely, the 50% degraded surrogate material. In addition, we recommend using the bed operational shear strength (τ_c) as it is more representative of the repository situation in which a drill penetrates through the degraded material thickness. Also as the value of τ_c is intermediate to τ_{so} and τ_{sc} , e.g., $\tau_{so} < \tau_c < \tau_{sc}$ it represents a value which is reasonable but conservative.

We therefore recommend a lower limit value for BOREHOLE : TAUFAIL of 1.50 Pa.

In addition, we recommend changing the distribution from log-uniform to uniform. The new distribution spans less than two orders of magnitude, i.e.

$$\log_{10}\left(\frac{77}{1.50}\right) = 1.71 \quad (7-1)$$

The use of a uniform distribution is appropriate when all that is known about a parameter is its range, as is the case here for TAUFAIL. The uniform distribution is the maximum entropy distribution under these circumstances. Log-uniform distributions are appropriate for parameters that span many orders of magnitudes (Tierney 1996).

Parameter statistics to be entered into the parameter database are given in Table 7-2.

Table 7-2. Statistics for the parameter BOREHOLE : TAUFAIL to be entered into the parameter database:

Minimum	1.50 Pa
Maximum	77 Pa
Distribution	Uniform
Mean	39.25 Pa
Median	39.25 Pa
Standard Deviation	21.79 Pa

8 References

Berglund, J.W. 1992. *Mechanisms Governing the Direct Removal of Wastes from the Waste Isolation Pilot Plant Repository Caused by Exploratory Drilling*. Sandia National Laboratories, Albuquerque, NM. SAND92-7295.

- Berglund, J.W. 1996. Effective shear resistance to erosion TAUFAIL. Memo to B.M. Butcher, October 28, 1996. Sandia National Laboratories, Carlsbad, NM. ERMS 247189.
- Buffington, J.M. 2007. Re: Critical shear strengths. E-mail sent to C. Herrick, February 22, 2007. ERMS 545763.
- Buffington, J.M. and D.R. Montgomery. 1997. A systematic analysis of eight decades of incipient motion studies, with special reference to gravel-bedded rivers. *Water Resources Research*, vol. 33, no. 8, pages 1993-2029. ERMS 545812.
- Butcher, B.M. 1994. A Model for Cuttings Release Waste Properties. Memorandum to distribution. January 6, 1994. Sandia National Laboratories, Albuquerque, NM. ERMS 309846.
- Butcher, B.M., S.W. Webb, J.W. Berglund, and P.R. Johnson. 1995. *Systems Prioritization Method – Iteration 2. Baseline Position Paper: Disposal Room and Cuttings Models, Vol. 1*. Sandia National Laboratories, Carlsbad, NM. ERMS 228729.
- Cao, Z., G. Pender, and J. Meng. 2006. Explicit formulation of the Shields diagram for incipient motion of sediment. *Journal of Hydraulic Engineering*, vol. 132, iss. 10, pp. 1097-1099. ERMS 545813.
- CTAC (Carlsbad Area Office Technical Assistance Contractor). 1997. *Expert Elicitation on WIPP Waste Particle Diameter Size Distribution(s) During the 10,000-year Regulatory Post-closure Period: Final Report*. U.S. Department of Energy – Carlsbad Area Office, Carlsbad, NM. ERMS 541365.
- Das, B.M. 2006. *Principles of Geotechnical Engineering*, 6th ed. Thomson, Ontario, Canada.
- DOE (U.S. Department of Energy). 1996. *Title 40 CFR Part 191 Compliance Certification Application for the Waste Isolation Pilot Plant*. DOE/CAO-1996-2184. October 1996.
- EPA (U.S. Environmental Protection Agency), 1998. *Technical Support Document for Section 194.23: Parameter Justification Report*. Docket A-93-02, V-B-14. ERMS 525159.
- Hansen, F.D. 2005. A Revisit of Waste Shear Strength. Sandia National Laboratories, Carlsbad, NM. ERMS 541354.
- Hansen, F.D., M.K. Knowles, T.W. Thompson, M. Gross, J.D. McLennan, J.F. Schatz. 1997. *Description and Evaluation of a Mechanistically Based Conceptual Model for Spall*. Sandia National Laboratories, Albuquerque, NM. SAND97-1369.
- Hansen, F.D., T.W. Pfeifle, and D.L. Lord. 2003. *Parameter Justification Report for DRSPALL*. Sandia National Laboratories, Albuquerque, NM. SAND2003-2930.
- Herrick, C.G., M. Riggins, and B.Y. Park. 2007. *Recommendation for the Lower Limit of the Waste Shear Strength (Parameter BOREHOLE : TAUFAIL), rev. 0*. Sandia National Laboratories, Carlsbad, NM. ERMS 546033.

Jepsen, R., J. Roberts, and W. Lick. 1997. Effects of bulk density on sediment erosion rates. *Water, Air, and Soil Pollution*, vol. 99, pp. 21-31. ERMS 252718.

Jepsen, R., J. Roberts, and W. Lick. 1998. Development and Testing of Waste Surrogate Materials for Critical Shear Stress. Sandia Contract AX-9022. Dept. of Mechanical and Environmental Engineering, University of California-Santa Barbara. ERMS 533809.

Julien, P.Y. 1998. *Erosion and Sedimentation*. Cambridge University Press, Cambridge, U.K.

Kirkes, R. and C.G. Herrick. 2006. Analysis plan for the modification of the waste shear strength parameter and direct brine release parameters: AP-131, rev. 0. Sandia National Laboratories, Carlsbad, NM. ERMS 545130.

Kruger, M. 1997. Performance assessment parameter values identified in EPA letters, dated April 17 and 25, 1997, to DOE. Docket A-93-02, II-I-33.

Mehta, A.J., T.M. Parchure, J.G. Dixit, and R. Ariathurai. 1982. Resuspension potential of deposited cohesive sediment beds. *Estuarine Comparisons*. V.S. Kenedy, ed. Academic Press, New York, N.Y. pp. 591-609. ERMS 545815.

Mellegard, K. 1998. Fabrication of Surrogate Waste Bricks for Erosion Studies: Laboratory Notebook (Volume 1 of 1). RSI Job 325 Task 20.1. Sandia National Laboratories Contract No. AG-4911. RESPEC, Rapid City, SD. ERMS 251625.

Parchure, T.M. and A.J. Mehta. 1985. Erosion of soft sediment deposits. *Journal of Hydraulic Engineering*, vol. 111, no. 10, 1308-1326. ERMS 545817.

Partheniades, E. 1962. *A Study of Erosion and Deposition of Cohesive Soils in Salt Water*. PhD thesis. University of California, Berkeley, California. ERMS 545818.

Partheniades, E. 1965. Erosion and deposition of cohesive soils. *Journal of the Hydraulics Division, Proceedings of the American Society of Civil Engineers*, vol. 91, no. HY1, pp. 105-139. ERMS 545819.

Partheniades, E. and R. E. Paaswell. 1970. Erodibility of Channels with Cohesive Boundary. *Journal of the Hydraulics Division, Proceedings of the American Society of Civil Engineers*, vol. 96, no. HY3, pp. 755-771. ERMS 241125.

Peake, T. 1997. Shear resistance to erosion (TAUFAIL). Facsimile to G. Basabilvazo. April 28, 1997. ERMS 545768.

Roberts, J., R. Jepsen, D. Gotthard, and W. Lick. 1998. Effects of particle size and bulk density on erosion on quartz particles. *Journal of Hydraulic Engineering*, vol. 124, no. 12, pp. 1261-1267. ERMS 252966.

Sargunam, A., P. Riley, K. Arulanandan, and R.B. Krone. 1973. Physico-chemical factors in erosion of cohesive soils. *Journal of the Hydraulics Division, Proceedings of the American Society of Civil Engineers*, vol. 99, no. HY3, 555-558. ERMS 241126

Simon, D.B. and F. Senturk. 1992. *Sediment Transport Technology: Water and Sediment Dynamics*. Sedimentation Engineering Manual No. 54. American Society of Civil Engineers, Water Resources Publication. Cited in Trovato (1997b).

Teeter, A.M. 1987. *Alcatraz Disposal Site Investigation. Report 3: San Francisco Bay-Alcatraz Disposal Site Erodibility*. Miscellaneous Paper HL-86-1. Department of the Army. Waterways Experimental Station, Corps of Engineers, Vicksburg, MS. AD Number A181837. ERMS 545820.

Tierney, M.S. 1996. Distributions. Sandia National Laboratories, Carlsbad, NM. ERMS 235268.

Trovato, E.R. 1997a. Letter to G. Dials (DOE), April 17. Office of Air and Radiation, U.S. Environmental Protection Agency, Washington, D.C. Docket A-93-02, II-I-25.

Trovato, E.R. 1997b. Letter to G. Dials (DOE), April 25. Office of Air and Radiation, U.S. Environmental Protection Agency, Washington, D.C. Docket A-93-02, II-I-27.

Wang, Y. 1997. Estimate WIPP waste particle sizes based on expert elicitation results: revision 1. Memorandum to M.S.Y. Chu and M.G. Marietta, Aug 5, 1997. Sandia National Laboratories, Albuquerque, NM. ERMS 246936.

Wang, Y. and K.W. Larson. 1997. Estimate waste critical shear stress for WIPP PA caving model. Sandia Memorandum to M.S.Y. Chu and M.G. Marietta, June 27, 1997. Sandia National Laboratories, Albuquerque, NM. ERMS 246696.

WIPP PA (WIPP Performance Assessment). 2004a. *Design Document for CUTTINGS_S (Version 6.00)*. Sandia National Laboratories, Carlsbad, NM. ERMS 537038.

WIPP PA (WIPP Performance Assessment). 2004b. *User's Manual for CUTTINGS_S (Version 6.00)*. Sandia National Laboratories, Carlsbad, NM. ERMS 537039.

WIPP PA (WIPP Performance Assessment). 2005a. *Addendum to the Design Document for CUTTINGS_S (Version 6.00)*. Sandia National Laboratories, Carlsbad, NM. ERMS 539236.

WIPP PA (WIPP Performance Assessment). 2005b. *Addendum to the User's Manual for CUTTINGS_S (Version 6.00)*. Sandia National Laboratories, Carlsbad, NM. ERMS 539238.

Herrick, Courtney Grant

From: Riggins, Michael
Sent: Thursday, June 21, 2007 7:15 AM
To: Herrick, Courtney Grant; Vugrin, Eric
Subject: RE: Signature authority needed

Importance: High

Eric,

I give signature authority to Eric Vugrin for all documents pertaining to the paper
"Recommendation for the Lower Limit of the Waste Shear Strength (Parameter BOREHOLE :
TAUFAIL) Rev. 1"

Mike Riggins, PhD
Sandia Nat'l Labs
Org 6711 - WIPP PA
(505) 234-0066 Carlsbad
(512) 482-0008 Austin
(505) 284-2730 Albuquerque
mriggi@sandia.gov

From: Herrick, Courtney Grant
Sent: Wednesday, June 20, 2007 2:28 PM
To: Riggins, Michael
Subject: Signature authority needed

Mike,

Please send someone signature authority for revision 1 of our analysis report.

Courtney